15. Petrology of Associated Igneous Rocks

By W. Ian Ridley

15 of 21

Volcanogenic Massive Sulfide Occurrence Model

Scientific Investigations Report 2010–5070–C

U.S. Department of the Interior
U.S. Geological Survey

U.S. Department of the Interior
KEN SALAZAR, Secretary

U.S. Geological Survey
Marcia K. McNutt, Director

U.S. Geological Survey, Reston, Virginia: 2012

Suggested citation:
Ridley, W. Ian, 2012, Petrology of associated igneous rocks in volcanogenic massive sulfide occurrence model: U.S. Geological Survey Scientific Investigations Report 2010–5070 –C, chap. 15, 32 p.

Contents

Figures

Tables

15. Petrology of Associated Igneous Rocks

By W. Ian Ridley

Importance of Igneous Rocks to Deposit Genesis

Volcanogenic massive sulfide deposits, by definition, are either hosted within or closely spatially associated with volcanic and subvolcanic intrusive rocks. Consequently, there is a well-documented genetic association between magmatism and development of VMS deposits (Lydon, 1988; Lowell and others, 1995, 2008; Franklin and others, 2005). Magmatism is a prerequisite in the following ways:

1. As a heat engine to drive deep hydrothermal flow systems (Maclennan, 2008), highlighted in modern systems by the association of melt-rich crustal regions of modern ridge systems and seafloor hydrothermal activity (Singh and others, 1999, 2006).

2. As a focus of hydrothermal circulation (Lowell and others, 2008). Subvolcanic intrusions act as "pinpoint" heat sources that focus descending fluids from recharge areas into narrow upflow and discharge zones. Models of heat and mass transport suggest that the hydrothermal flow system has an aspect ratio of approximately one. Focused flow is required to produce an ore deposit at the seafloor and subseafloor (Hannington and others, 2005) and is consistent with the alteration patterns observed in ancient VMS deposits (Large and others, 2001c).

3. As a source of chemical components to hydrothermal systems (Seyfried and others, 1999; Openholzner and others, 2003; Yang and Scott, 2006). Although it is generally accepted that metals are sourced from hydrothermal fluid/rock interactions along the fluid-flow path, metals may also be added from magmatic fluids and gases associated with the late stages of magmatic crystallization, as inferred in the current mineralizing system on Papua New Guinea (Gemmell and others, 2004).

Rock Names

Rock names and rock associations that are commonly found with VMS deposits can be found in Le Maitre (2002) and the various figures therein.

Rock Associations

The lithogeochemistry of volcanic rock associations generally can be applied to specific tectonic settings. Here, the rock associations are classified as mafic, bimodal-mafic, siliciclastic-mafic, bimodal-felsic, and siliciclastic-felsic. The identification of specific tectonic settings for VMS deposits is referenced to the lithogeochemistry of volcanics in modern tectonic settings (Pearce and Cann, 1973; Pearce, 1995; Pearce and Peate, 1995; Piercey, 2009). It is common to observe more than one lithologic association in large VMS districts; for instance, the giant Bathurst district contains deposits that are associated with bimodal-mafic and siliciclastic-felsic associations (Goodfellow and others, 2003). Although these associations form a reasonable descriptive system, gradations between associations are common depending upon the scale of description (regional versus local). Mapping of VMS deposits often identifies felsic lava flows and subvolcanic felsic intrusions as the local-scale igneous associations (Large and others, 2001a, c; Monecke and others, 2006). The details of volcanic architecture and their volcanologic implications can be found in Chapter 5 (Morgan and Schulz, this volume); they have also been discussed in detail by Cas (1992). Rock associations are important features of VMS deposits because: (1) at the local scale, they identify sources of heat that drive hydrothermal circulation and local sources of magmatic metals and acidity; (2) at the more regional scale, they provide information on sources of metals that may give a VMS deposit its specific metal signature (Large, 1992; Stolz and Large, 1992); and (3) they provide a mechanism for the rapid burial of a massive sulfide deposit, for example, the geologically instantaneous emplacement of volcanoclastic turbidites.

Mafic-Ultramafic Association

The mafic-ultramafic association represents VMS deposits that are spatially connected with lithologies dominated by basaltic and (or) ultramafic rocks. The latter are rare occurrences in the rock record, for example, Greens Creek (Duke and others, in press), and their genetic relationship to ore is unclear. In Archean greenstone belts, VMS deposits may be associated with komatiite lavas. The VMS mafic-ultramafic associations dominated by basaltic rocks are found in the upper parts of obducted ophiolite complexes, for example,

Oman, Troodos, and Turner-Albright. In the modern oceans, the mafic association is found in two specific settings: mid-ocean ridges and mature back-arc basins. Hydrothermal activity spatially associated with ultramafic rocks, usually serpentinites, has been observed at several localities proximal to the Mid-Atlantic Ridge, for example, Lost City (Kelley and others, 2007), Logachev (Krasnov and others, 1995a), and the Gakkel Ridge (Edmonds and others, 2003). These hydrothermal systems are associated with oceanic core complexes formed during attenuation of the ocean crust at magma starved ridges. Although serpentinization is an exothermic process, which may be a significant source of heat in low-temperature (<100 °C) hydrothermal systems, it is likely the heat engine for high-temperature (350–450 °C) hydrothermal circulation is driven by subjacent gabbroic intrusives (Alt and Shanks, 2003; Allen and Seyfried, 2004; Alt and others, 2008). Further, Allen and Seyfried (2004) have argued that the geochemistry of the vent fluids at the Lost City low-temperature hydrothermal system indicates they are spent and cooled higher temperature fluids.

Olivine tholeiites are the common volcanic rock type found at mid-ocean ridges (MORs) and are collectively known as mid-ocean ridge basalts (MORBs). They are further divided into DMORB (depleted), NMORB (normal), TMORB (transitional), and EMORB (enriched) depending principally on their K/Ti ratios and incompatible element compositions. Many sites of active and extinct hydrothermal sulfide accumulation have been discovered along the mid-ocean ridge system, especially along the northern East Pacific Rise, but almost all have grades and tonnages that would be uneconomic if preserved in the rock record. An exception is the 3.9-Mt TAG deposit on the Mid-Atlantic Ridge (Hannington and others, 1998), but deposits with grades and tonnages equivalent to the larger VMS deposits have yet to be found at either mid-ocean ridge or back-arc basin sites.

It should also be noted that at some MOR sites that are regionally dominated by mafic lithologies, there exist more localized but still volumetrically substantial accumulations of basaltic andesite, andesite, dacite, and rhyolite. Examples include the overlapping spreading center at 9 °N on the East Pacific Rise (Wanless and others, 2010), the Galapagos spreading center (Embley and others, 1988; Perfit and others, 1999), and the southern Juan de Fuca Ridge (Cotsonika and others, 2005). In these environments, the more evolved igneous rock types are associated with hydrothermal activity and are the product of fractional crystallization of MORB and assimilation due to anatexis of shallow, hydrated basaltic crust. Consequently, in the absence of other information, the presence of more evolved rocks in an otherwise mafic association does not eliminate the possibility of an open-ocean setting.

The presence of the mafic-ultramafic association in back-arc basins is a function of proximity to the seaward island arc and is most clearly observed in mature back-arc basins that have well-organized spreading, for instance, east Scotia Sea, Lau Basin, and the Mariana Trough. The chemistry of basalts associated with island-arc systems is a complex function of mantle chemistry and interactions between the mantle and fluids/melts ascending from the subducting slab (fig. 15–1).

In these settings, the hydrothermal systems are distinct from mid-ocean ridge systems in having much higher volatile contents that reflect the general, although not universal, volatile-rich nature of the associated volcanics and presumed subvolcanic intrusions (Gamo and others, 2006). The higher volatile contents also result in hydrothermal fluids that have pH values as low as 2, substantially less than found in mid-ocean ridge hydrothermal fluids and probably related to disproportionation of dissolved SO_2. A variety of basalts have been identified in back-arc basins, including MORBs that are chemically indistinguishable from those observed in open-ocean settings, and they range in composition from DMORB (central Lau Basin) to EMORB (north Fiji Basin). Importantly, a basalt type unique to the back-arc setting has been recognized and termed back-arc basin basalt (BABB). The latter has unique trace element signatures, particularly depletion in high field strength elements reflecting the subduction environment, and includes both depleted and enriched varieties (Pearce and Stern, 2006).

Siliciclastic-Mafic Association

This association is defined as subequal volumes of siliciclastic, sometimes pelitic, sediments and mafic, occasionally ultramafic, volcanic rocks. The mafic component is largely composed of volcanics with MORB-like affinities. The deposits of the Besshi district are the classic examples, but other examples include Windy Craggy and the small Hart River and Ice deposits in Canada and Greens Creek in the United States. Modern analogs include open-ocean spreading ridges with active hydrothermal systems that are sufficiently proximal to continents to receive significant volumes of sediment, such as observed at Escanaba Trough on the Gorda Ridge, Middle Valley on the northern Juan de Fuca Ridge, and Guaymas Basin in the Gulf of California. The relationship of the siliciliclastic component to generation of VMS deposits is tenuous. Most VMS deposits form in relatively deep water (>1 km), which many workers propose inhibits exsolution of volatiles and formation of fragmental rocks, other than autobreccias, and results in a proximal volcanic stratigraphy that is dominated by lava flows. However, this interpretation of a nonfragmental requirement is controversial. Most silicic volcanoclastics appear to be redeposited lithologies (Monecke and others, 2006) sourced at shallow depths and emplaced in turbidity currents.

Bimodal-Mafic Association

This association is defined as VMS deposits that are principally correlated with mafic lithologies, but with up to 25 percent felsic rocks. Examples include the giant Kidd Creek, Flin Flon, Ruttan, and Bathurst deposits in Canada; the small Sumdum and Bald Mountain deposits in the United States

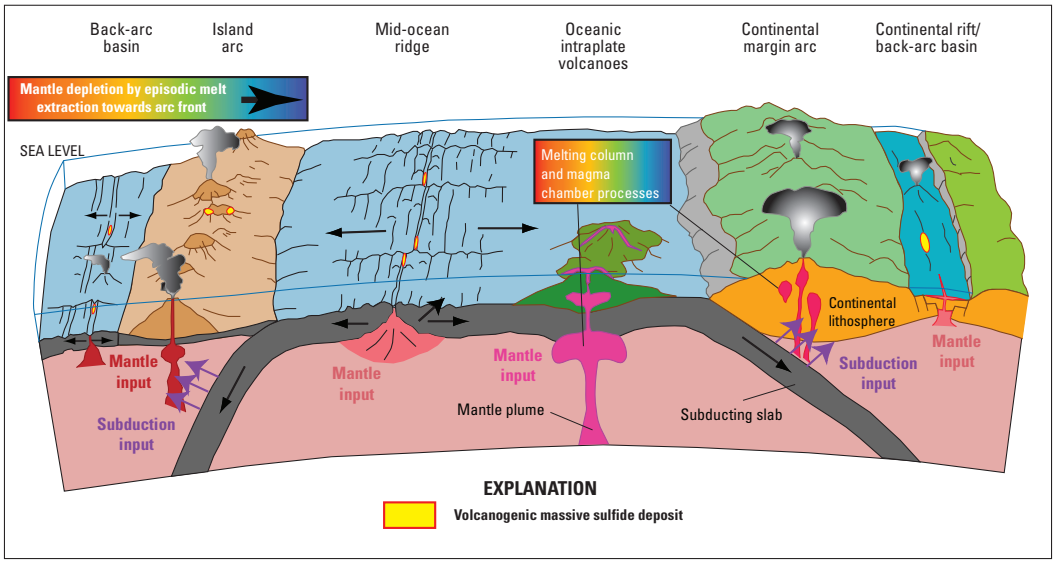

Figure 15–1. Schematic diagram showing the principal components and processes involved in the production of island-arc and back-arc volcanics that are major lithostratigraphic units associated with volcanogenic massive sulfide deposits. Subduction input includes (1) fluids released at shallow depths due to dehydration reactions, and (2) silicate melts released during partial melting at greater depths. These two processes metasomatize the overlaying mantle, adding distinct trace-element assemblages. Movement of the asthenosphere is in response to the subduction process and may involve arc-parallel and arc-oblique movement. Two different mantle domains have been recognized in the western Pacific arcs—"Indian" and "Pacific"—based on isotopic systematics (Klein and others, 1988). Mantle melt extraction at shallow levels and subsequent mixing and fractionation produces a wide variety of volcanics at the surface, most of which are characterized by their hydrous nature. Island-arc volcanics are fundamentally different from back-arc volcanics because of the different inputs from the subducting oceanic crust. Modified from Pearce and Stern (2006).

(Schultz and Ayuso, 2003); and the Eulaminna deposit in Australia. The important criterion is that the felsic rocks commonly host the deposits (Barrie and Hannington, 1999; Galley and others, 2007). The mafic component may include MORB-type basalts, BABB-type basalts, and boninites that are associated with rhyolites. The tectonic setting is either:

a. formed in a back-arc basin that is proximal to an island arc, for instance, the East Lau spreading center, north and south Mariana Trough, and the Kermadec Arc. The volcanics have a strong subduction component and (or) include felsic volcanics formed by partial melting of the root zones of a mature arc;

b. formed in a fore-arc setting where the initiation of the volcanic front is dominated by basalts with minor components of more fractionated felsic volcanics (Jakes and White, 1971); or

c. formed in an epicontinental arc setting in which the felsic components are sourced within the continental crust.

Bimodal-Felsic Association

This association is defined as VMS deposits that are principally correlated with felsic volcanics with a minor component of mafic volcanics. Examples include the deposits of the Kuroko and the Buchans districts. The minor mafic component may include MORB-like basalts, often with EMORB chemical signatures, and alkalic basalts that have ocean-island basalt (OIB) signatures and may also include shoshonites. This association is frequently associated with epicontinental arc environments. The felsic component may include andesites, dacites, and rhyolites but is often dominated by rhyolite that often has calc-alkaline affinities, for example, Mount Read deposits, Tasmania.

In modern arc settings, the bimodality is often developed at the mature stage of volcanism, such as with the Aleutian and Melanesian arcs, and the abundant rhyolites are considered to form by partial melting of the deeper, basaltic parts of the volcanic superstructure. The presence of highly alkalic magmas, particularly the eruption of shoshonites, is usually associated

with late-stage, low-volume volcanism, as observed in New Guinea. Bimodal felsic associations also may form during the incipient stages of back-arc basin development, where volcanics with arclike affinities are associated with alkalic magmas produced by lithospheric melting with a progression toward MORB-like magmas as the crust becomes attenuated.

Siliciclastic-Felsic Association

This association has a minor component of mafic volcanics, which may be as little as 20 percent, as observed in some of the Bathurst district deposits. The geochemistry of felsic volcanics, which include submarine pyroclastic and epiclastic flows (turbidites), crystal tuffs of dacitic, and rhyolitic composition, indicates a source by incorporation of variable amounts of continental crust with the heat sources being basaltic to gabbroic magmas that were ponded at a density barrier within the thick crust. This association also hosts major VMS deposits, such as the Iberian Pyrite Belt and parts of the Bathurst district. In the United States, VMS deposits at Crandon, Red Ledge, and Iron Mountain have this lithologic association.

Mineralogy

The primary mineralogy of volcanic rocks reflects crystallization during magmatic cooling over a temperature interval from approximately 1,300 to 900 °C. However, during interaction with hydrothermal fluids at much lower temperatures (450–350 °C and lower), the primary minerals and volcanic glass are destabilized. Consequently, rocks that compose the volcanic stratigraphy associated with VMS deposits, particularly in the footwall, are invariably, and pervasively, altered. In addition, secondary phases may be produced during postore metamorphic reactions. The primary magmatic minerals provide a feedstock and a sink of major, minor, and trace elements to circulating hydrothermal fluids. The major-element compositions of the principal primary minerals and the more common mineral-fluid ion exchanges involving major, minor, and trace elements are shown in table 15–1.

The pristine rocks also may contain glass, varying in amount from an interstitial component to a major constituent. The glass can be highly variable in composition, from ultramafic through basaltic to rhyolitic, with a wide suite of incompatible trace elements. Glass is highly unstable and is usually the first primary phase to be altered under hydrothermal conditions. In lithologies dominated by basaltic and andesitic rocks, glass is likely to be a minor component and contribute only a minor amount of trace elements to circulating fluids. However, more felsic rocks, such as dacites and rhyolites, may have a major glassy component.

Textures and Structures

The primary volcanic textures of igneous rocks associated with VMS deposits are usually overprinted during fluid/rock interactions. However, textures play an important role, along with fluid chemistry and temperature, in determining the rate at which the various primary phases are destabilized. Based on examination of volcanics associated with modern marine sulfide deposits, there exists a wide range of crystallinities from entirely crystalline (holocrystalline) through intermediate crystallinities (hypocrystalline or hypohyaline) to entirely glassy (holohyaline). Some common volcanic textures are described in table 15–2.

The structures of volcanic rocks associated with VMS deposits are highly variable and are a function of composition and submarine structural setting. Most volcanic successions are emplaced in rift settings that are dominated by island-arc or continental-margin-arc environments and may involve back-arc and intra-arc rifting. Siliciclastic-mafic-type deposits have a large component of clastic sediments mixed with basaltic dikes and sills and form on rifted open-ocean ridges proximal to a continental source of sediment. Modern settings include Middle Valley, Escanaba Trough, and Guaymas Basin. Particularly important is the relationship between composition, viscosity, and dissolved gas contents, which determine the explosive potential of magma. Apart from VMS deposits formed in shallow (<500 m) submarine settings, the volcanic architecture is dominated by flows and related autobreccias with spatially associated volcanoclastic rocks being derived from shallow, distal environments that may be either submarine or subaerial. In mafic-associated VMS deposits, the basalts are usually thin lava flows (pillows, sheet flows, and hummocky flows) with a large aspect ratio, excepting cases where ponding against neovolcanic faults produces thickened lava lakes. In VMS deposits associated principally with felsic volcanics, the latter are dominantly lava flows with flow domes, small aspect ratios, peperites, and autoclastic breccias. As described above, pumice-rich breccias, hyaloclastites, lapilli tuffs, crystal tuffs, vitric tuffs, ash fall deposits, and ash flows (ignimbrites) generally have distal, shallow sources. In stacked VMS deposits, intercalated volcanoclastics provide enhanced porosity and permeability resulting in diffuse fluid flow, whereas more focused flow may be related to fracture porosity provided by flows and flow domes. In some cases, subvolcanic intrusions may be exposed and are usually quartz-feldspar porphyries. The variations and types of structures that develop depend largely on the specific volcanic environment of deposition. Caldera settings have been proposed for some Kuroko deposits (Ohmoto and Takahashi, 1983), although these cannot be formed by explosive release of subvolcanic magma in the classic sense of central volcano collapse, and

Table 15–1. Major and trace element composition of major minerals observed in igneous rocks associated with modern seafloor massive sulfides in a variety of settings.

[PGE, platinum group elements; REE, rare earth elements; Ag, silver; Al, aluminum; As, arsenic; Au, gold; Ba, barium; Be, beryllium; Ca, calcium; Cl, chlorine; Co, cobalt; Cr, chromium; Cu, copper; Eu, europium; F, fluorine; Fe, iron; In, indium; K, potassium; Li, lithium; Mg, magnesium; Mn, manganese; Na, sodium; Ni, nickel; Pb, lead; Rb, rubidium; S, sulfur; Sc, scandium; Si, silicon; Sr, strontium; Ti, titanium; V, vanadium; Zn, zinc]

Minerals	Major elements	Trace elements
Plagioclase	$CaAl_2Si_2O_8$ (anorthite) – $NaAlSi_3O_8$ (albite) solid solution	Na+, Al+++, Ca++, Sr++, Ba++, Eu++
K-Feldspar	$KAlSi_3O_8$ (orthoclase, sanidine)	Li+, Al+++, K+, Rb+, Ba++, REE
Olivine	Mg_2SiO_4 (forsterite) – Fe2SiO4 (fayalite) solid solution	Mg++, Fe++, Co++, Ni++
Clinopyroxene	$CaSiO_3$ (wollastonite) – $MgSiO_3$ (enstatite) – $FeSiO_4$ (ferrosilite) solid solution	Mg++, Al+++, Ca++, Sc++, Ti++++, Cr+++, Mn++, Fe++, REE
Orthopyroxene	$MgSiO_4$ (enstatite) – $FeSiO_4$ (ferrosilite) solid solution	Mg++, Al+++, Mn++, Fe++, Co++, Zn++
Amphibole	$(Ca, Na)(Ca, Fe_2+, Mg, Na)_2(Al, Fe^{2}+, Fe^{3+}, Mg)_5(Al, Si, Ti)_8O_{22}(OH, F, Cl)_2$ (general formula)	F-, Cl-, Na+, Mg++, Al+++, Ca++, Ti++++, V+++, Cr+++, Mn++, Fe++, Fe+++, Co++, Ni++, Zn++
Mica	$K(FE^{2}+)_3(Al, Fe^{3+})Si_3O_{10}(OH, F, Cl)_2$ (biotite) – $KMg_3AlSi_3O_{10}(OH, F, Cl)_2$ (phlogopite) solid solution	Be++,F-, Mg++, Al+++, Cl-, K+, Fe++, Fe+++, V+++, Zn++
White mica	$KAl_2(Si_3Al)O_{10}(OH, F, Cl)_2$ (muscovite)	Li+, Be++, F-, Al+++, Cl-, K+
Spinel	$Fe^{2+}Fe_2^{3+}O_4$ (magnetite) – $MgFe_2^{3+}O_4$ (magnesioferrite) – $Fe^{2+}Cr_2O_4$ (chromite) – $MgAl_2O_4$ (spinel) solid solution	Mg++, Al+++, Ti++++, V+++, Cr+++, Mn++, Mn+++, Fe++, Fe+++, Co++, Ni++
Oxide	$FeTiO_3$ (ilmenite) – $MgTiO_3$ (geikielite) solid solution	Mg++, Si++++, Ti++++, Mn++, Fe++
Sulfide	(Fe, Ni)S (monosulfide solid solution). (Fe, Ni, Cu)S (intermediate solid solution). FeS_2 (pyrite). $Fe_{1-x}S$ (pyrrhotite)	S--, Fe++, Co++, Ni++, Cu++, Zn++, As---, In+++, Ag+, Au+++, rare metals, PGE, Pb++
Notes:	Silicates are also a major source of silica to solution. Metals may be carried as either chloride or bisulfide complexes.	

well-defined caldera structures have not been mapped. More detailed descriptions of volcanic architecture can be found in Chapter 5.

Petrochemistry

Many different schemes for the classification of igneous rocks have been proposed (Philpotts, 1990). Two that are commonly used and quoted are shown in figure 15–2.

Major-Element Geochemistry

The major-element chemistry of volcanic rocks associated with VMS deposits is determined by a combination of source composition, temperature and pressure (mantle and crustal regimes), and subsequent fractional crystallization and (or) assimilation. Generally, the major basaltic series are divided into tholeiitic (MORB, BABB), calc-alkalic (island-arc basalt [IAB]), and alkalic (OIB), but island-arc settings also include the boninite and shoshonite series. The major-element compositions of different types of basaltic rocks associated with VMS deposits are found in table 15–3 and more evolved rocks in table 15–4.

The major-element composition of altered volcanics reflects the degree of alteration and alteration mineralogy and is a useful guide to the proximity of ore. For instance, Offler and Whitford (1992) show that the alteration halo around the Que River deposit, Tasmania, can be mapped using major-element compositions and associated mineral chemistry. Large and others (2001b) developed the “alteration box plot” that employs two major element alteration indices: the Ishikawa alteration index:

$$100K_2O+MgO)/(K_2O+MgO+Na_2O+CaO),$$

and a chlorite-carbonate-pyrite index or CCPI:

$$100(MgO+FeO)/(MgO+FeO+Na_2O+K_2O),$$

which they modify from Lentz (1999). This scheme: (1) can generally be used to distinguish alteration effects from subsequent metamorphic overprint; (2) cannot recognize quartz gangue mineralization; (3) is mainly useful for felsic versus mafic volcanics; and (4) cannot be used for altered clastic sedimentary rocks.

Trace-Element Geochemistry

An overview of the lithogeochemistry, including trace-element geochemistry, of volcanic rocks associated with VMS deposits can be found in Piercey (2009). Trace elements have played a fundamental role in the classification of igneous rocks from a wide variety of tectonic settings, and their geochemical behavior has been used extensively to identify and separate the geologic processes active in the production of the

Table 15–2. Common textures observed in pristine igneous rocks associated with modern seafloor massive sulfides.

Name	Desciption
Hyaline	A completely glassy rock that may contain minor quenched crystals (crystallites). Commonly observed in submarine volcanics as quenched surfaces in basalts, basaltic andesites and andesites. Glass may make up a large volume of submarine and terrestrial evolved volcanics (dacites, rhyolites) if the melts are relatively dry. These latter volcanics often display distinct banding due to differences in: (a) crystallite abundances and orientations; (b) degree of devitrification; (c) degree of spherulite formation. Glass may also be the main product of submarine and terrestrial fire fountaining and welded and unwelded rhyolite tuffs. In the case of rhyolitic tuffs the texture is unwelded if the glass fragments are not welded together and are commonly found in a matrix of very fine grained glass (ash). In the case of welded tuffs the rock often has a laminated appearance due to extreme compaction and welding of original pumice fragments. The regular alignment of flattened pumice produces a texture known as eutaxitic.
Hypocrystalline	A partly crystalline rock that shows distinct differences in granularity due to presence of both crystals and glass. These rocks are often called vitrophyres or pitchstones with the modifying terms of the main phenocryst phases, for example, plagioclase-augite vitrophyre. In some cases the glass may have severely devitrified if it contains substantial dissolved water
Holocrystalline	A completely crystalline rock that may be equigranular or porphyritic. Equigranular rocks may be cryptocrystalline (individual crystals are submicroscopic) or microcrystalline (individual crystals are microscopic) or phaneritic (individual crystals can be discerned by eye). Equigranular rocks may be: (a) intersertal (hyalophitic,subophitic, ophitic), in which plagioclase is partly or completely surrounded by pyroxene and (or) olivine; (b) intergranular, in which one mineral phase dominates and other phases fill in the spaces between this phase; (c) trachytic, in which small feldspar crystals are aligned in a distinct flow texture. A variety is trachytoidal in which the feldspar crystals are larger yet still aligned in a flow pattern. Despite the name, these flow textures can be observed in rocks from basaltic to rhyolitic.
Cavity textures	A variety of cavity textures may also exist that include vesicular textures due to presence of irregular holes (vesicles) due to exsolution of a gas phase during magmatic cooling, amygdaloidal textures in which former vesicles are filled by late-magmatic or post-magmatic minerals (commonly carbonates, zeolites, quartz). In some coarser rocks the irregular-shaped gas cavities may be filled with late-magmatic, euhedral crystals and the texture is termed miarolitic.
Note:	The various textures of igneous rocks are important in determining the extent to which individual minerals react with percolating hydrotherm fluids. In turn, this determines the interchange of metals and other elements between the rock and the fluid.

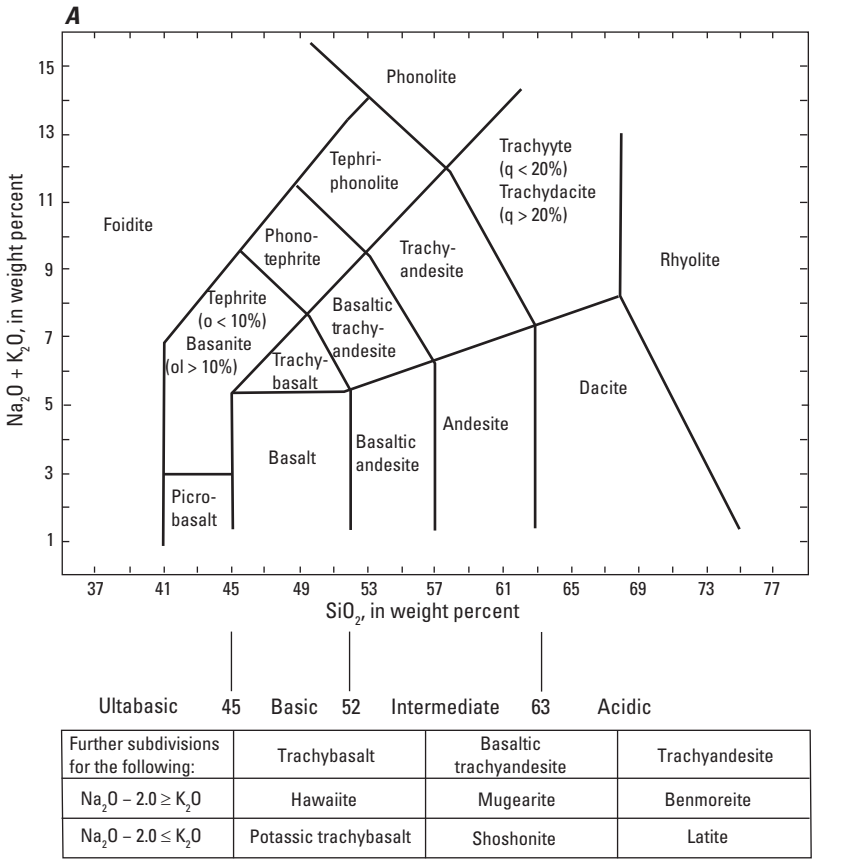

Further subdivisions for the following:	Trachybasalt	Basaltic trachyandesite	Trachyandesite
$Na_2O - 2.0 \geq K_2O$	Hawaiite	Mugearite	Benmoreite
$Na_2O - 2.0 \leq K_2O$	Potassic trachybasalt	Shoshonite	Latite

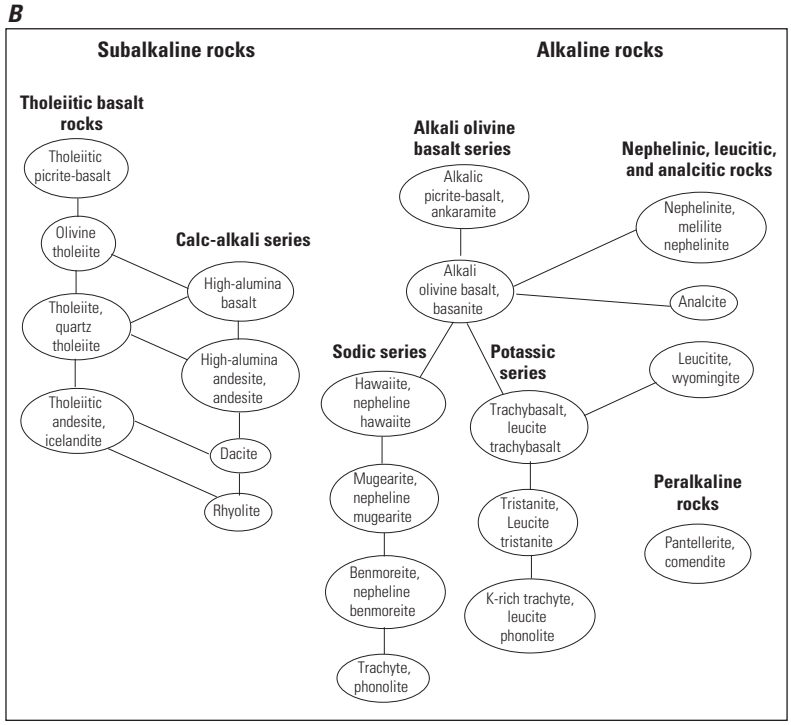

Figure 15–2. Two classifications of common igneous rocks. *A*, Total alkali ($N_2O + K_2O$) versus silica (SiO_2), or TAS, classification system. After Le Maitre (2002). *B*, Classification based on general chemical characteristics, with lines connecting commonly associated rocks. After Irvine and Baragar (1971).

Table 15–3. Average major element composition of basaltic rocks associated with volcanogenic massive sulfide deposits.

[DMORB, depleted mid-ocean ridge basalt; NMORB, normal mid-ocean ridge basalt; TMORB, transitional mid-ocean ridge basalt; EMORB, enriched mid-ocean ridge basalt; BABB, back-arc basin basalt; IAB, island-arc basin basalt. K/Ti = K_2O*100/TiO_2; Mg# = molar MgO/[MgO + FeO (Total)]. Data sources: IAB, Shoshonite from Jakes and White (1971); MORB data from northern East Pacific Rise; BABB data from Fiji and Lau Basins; Data from PetDB, Petrologic Database of the Ocean Floor (www.petdb.org)]

	DMORB[1]	NMORB[2]	TMORB[3]	EMORB[4]	BABB[5]	BABB[6]	BABB[7]	BABB[8]	IAB	Shoshonite
SiO_2	50.32	50.17	50.34	50.56	49.09	49.15	49.04	50.40	50.59	53.74
TiO_2	1.17	1.19	1.22	1.24	1.29	1.16	0.99	0.99	1.05	1.05
Al_2O_3	15.47	15.79	16.02	15.40	16.83	16.30	16.55	16.52	16.29	15.84
FeO (Total)	9.09	8.28	8.69	8.45	9.59	9.32	8.14	8.78	8.37	7.77
MnO	0.18	0.16	0.15	0.16	0.11	0.14	0.15	0.17	0.17	0.11
MgO	9.14	8.33	8.12	8.58	8.91	8.85	8.70	8.42	8.96	6.36
CaO	11.54	12.07	11.99	11.83	12.46	12.37	12.88	11.08	9.50	7.90
Na_2O	2.43	2.45	2.44	2.41	2.61	2.37	2.36	2.94	2.89	2.38
K2O	0.05	0.10	0.18	0.38	0.05	0.09	0.14	0.21	1.07	2.57
P_2O_5	0.12	0.11	0.13	0.16	0.16	0.14	0.08	0.13	0.21	0.54
K/Ti	3.7	8.1	15.0	29.7	4.0	7.4	14.1	21.1	20.0	51.4
Mg#	63.7	62.4	63.5	64.1	62.6	63.0	65.7	63.0	65.8	60.0

[1] DMORB: K/Ti <5; Mg# >60

[2] NMORB: K/Ti 5–11.5; Mg# >60

[3] TMORB: K/Ti 11.5–20; Mg# >60

[4] EMORB: K/Ti > 20; Mg# >60

[5] BABB with K/Ti < 5; Mg# >60

[6] BABB with K/Ti 5–11.5; Mg# >60

[7] BABB with K/Ti 11.5–20; Mg# >60

[8] BABB with K/Ti >20; Mg# >60

Table 15–4. Major element compositions of various volcanic rock series associated with volcanogenic massive sulfide deposits.

[MORB, Mid-ocean ridge basalt; NMORB, normal mid-ocean ridge basalt; n.d., no data; Al, aluminum]

	Boninite series[1]				MORB series[2]				Calc-alkaline series[3]		
	Boninite	Andesite	Dacite	Rhyolite	NMORB	Andesite	Dacite	High-Al basalt	Andesite	Dacite	Rhyolite
SiO_2	56.45	59.50	66.88	66.88	50.17	56.82	65.08	50.59	59.64	66.80	70.70
TiO_2	0.10	0.20	0.20	0.20	1.19	1.71	0.83	1.05	0.76	0.23	0.30
Al_2O_3	13.59	13.91	10.64	10.64	15.79	13.64	12.91	16.29	17.38	18.24	13.40
FeO (total)	7.82	7.72	4.54	4.54	8.28	10.13	6.81	8.37	5.00	2.14	3.50
MnO	0.10	0.11	0.07	0.07	0.16	0.19	0.12	0.17	0.09	0.06	0.30
MgO	5.40	3.04	0.43	0.43	8.33	3.09	0.8	8.96	3.95	1.50	0.05
CaO	9.19	7.63	3.04	3.04	12.07	6.55	3.16	9.50	5.93	3.17	2.80
Na_2O	2.09	2.57	3.39	3.39	2.45	4.12	4.81	2.89	4.40	4.97	4.90
K_2O	0.52	0.56	0.97	0.97	0.10	0.68	1.34	1.07	2.04	1.92	2.00
P_2O_5	n.d.	n.d.	n.d.	n.d.	0.11	0.23	0.19	0.21	0.28	0.09	0.01
K/Ti	544.44	273.40	483.75	506.25	8.11	39.72	161.45	101.90	268.42	834.78	666.67
Mg#	55.10	41.22	14.22	14.22	62.40	35.47	17.45	65.83	58.71	55.79	2.51

[1] Dobson and others (2006)

[2] V.D. Wanless, Woods Hole Oceanographic Institution, unpublished data (2009)

[3] Jakes and White (1971); Baker (1982)

[4] Ridley (1970); Chester and others (1985)

Table 15–4. Major element compositions of various volcanic rock series associated with volcanogenic massive sulfide deposits.—Continued

[MORB, Mid-ocean ridge basalt; NMORB, normal mid-ocean ridge basalt; n.d., no data; Al, aluminum]

	Shoshonite series[3]			Ocean island series[4]				
	Shoshonite	Latite	Basanite	Alkali olivine basalt	Hawaiite	Mugearite	Benmorite	Phonolite
SiO_2	53.74	59.27	44.22	48.04	47.21	56.36	60.95	62.08
TiO_2	1.05	0.56	12.74	1.47	1.62	1.71	1.44	0.98
Al_2O_3	15.84	15.90	2.93	15.35	16.50	15.37	17.62	16.32
FeO (total)	7.77	5.18	11.70	9.26	10.43	9.24	4.69	3.68
MnO	0.11	0.10	0.14	0.18	0.21	0.16	0.14	0.10
MgO	6.36	5.45	11.85	9.74	6.23	3.07	1.19	0.49
CaO	7.90	5.90	10.86	9.52	11.06	6.36	3.92	1.21
Na_2O	2.38	2.67	3.05	3.80	3.20	4.18	5.66	7.11
K_2O	2.57	2.68	1.01	0.65	1.76	2.11	2.77	5.45
P_2O_5	0.54	0.41	0.61	0.37	0.51	0.69	0.41	0.13
K/Ti	244.76	478.57	7.93	44.22	108.64	123.39	192.36	556.12
Mg#	59.57	65.44	64.58	65.44	51.81	37.42	31.35	19.33

various rock series that are associated with VMS deposits. One group of trace elements is particularly useful; the incompatible or lithophile trace elements that have a strong affinity for the melt phase during partial melting and fractional crystallization. Some of these elements also show chalcophilic (sulfur-seeking) behavior. The group includes the elements Li, Be, B, Sc, V, Cr, Rb, Sr, Cs, Ba, Nb, W, Pb, U, and Th. Some lithophile trace elements, such as Rb, Cs, and U, are mobile during post-emplacement weathering, diagenesis, metasomatism, and metamorphism. They may exhibit open system behavior and be selectively redistributed within the volcanic stratigraphy or lost completely.

It is common to separate out two subsets of incompatible elements: the high field strength elements (HFSE) and the rare earth elements (REE). The HFSE include Y, Zr, Hf, Nb, Ta, and the major element Ti. They are characterized by very similar geochemical behavior, are highly insoluble in aqueous fluids, and hence tend to be very immobile. The REE are the elemental series between La and Lu, and, except for Eu and in some cases Ce, behave as a coherent group of elements that is also substantially insoluble in aqueous fluids, excepting carbonate waters where they can form soluble and, hence, mobile carbonate species. The HFSE and REE are particularly useful because their immobility and fluid-insoluble nature results in: (1) a tendency to retain protolith geochemical characteristics that may prove useful to determine tectonic setting (fig. 15–2) (Dusel-Bacon and others, 2004; Piercey, 2009); and (2) a method to separate mantle processes from subduction slab processes. Many VMS studies use HFSE and REE to identify protolith provenance, for example, Whitford and Ashley (1992).

A useful graphical representation of trace-element abundances is the use of the so-called binary "spider diagram," an extension of the familiar REE-normalized abundance diagram. Each individual pattern is called a "spidergram" and is constructed by plotting an array of trace elements on the X-axis in order of decreasing incompatibility against elemental abundances on the Y-axis. The latter can be adjusted to a variety of normalizing values, depending upon the problem at hand, for example, primordial mantle, chondrites, MORB, average upper crust, North American shale (fig. 15–4).

Piercey (2009) has extended the spidergram to include the compatible elements Al, V, and Sc that may also be relatively immobile during alteration. Pearce and Stern (2006) have shown that normalization to MORB abundances and then renormalizing, so that $YB_N = 1$, is particularly useful in describing volcanic rocks in the various tectonic settings that host VMS deposits, especially those settings that involve suprasubduction and back-arc settings (fig. 15–4). Pearce and Stern (2006) have used trace elements to show that back-arc basins actually contain not only BABB volcanics, but also basalts that closely resemble the spectrum of compositions found at ocean-ridge systems, that is, DMORB to EMORB. These basalts must have depleted mantle sources that are geochemically similar to mantle underlying mid-ocean ridge magmatic systems. In contrast, spidergrams for BABB show much more element-to-element variability due to the influence of the subducting slab, for example, anomalous abundances of K, Ba, and Pb.

Spidergrams are useful in separating out the effects of mantle geochemistry, for instance, use of the Nb/Yb ratio (fig. 15–3). Discussions regarding trace-element behavior can be quite nuanced (Langmuir and others, 2006; Pearce and Stern, 2006), but some generalizations can be made. The geochemistry of back-arc basin basalts (BABB) is primarily determined by chemical interactions between mantle and fluids and (or) melts generated within the subducting slab. These interactions tend to decrease as a function of distance of the back-arc spreading system from the island-arc system. Secondarily, the geochemistry is determined by fractional crystallization and by assimilation, the latter being also a function of distance from the arc or an extending continental margin.

Besides their usefulness in petrogenetic studies, trace elements in VMS protoliths are an important source of cations and anions to circulating hydrothermal fluid. In particular, metals are efficiently leached from volcanic rocks at temperatures in excess of 300 °C (Seyfried and others, 1999, see Chapter 13, this report).

Transition element (Cr, V, Ni, Co, Cu) abundances decrease as a function of increasing silica content in all magma series (alkalic, tholeiitic, and calc-alkaline), whereas Pb concentrations increase. Generally, the concentration of transition metals in IAB (average 105 ppm Cu, 74 ppm Zn) and MORB (average 71 ppm Cu, 84 ppm Zn) is substantial (fig. 15–5) (Stanton, 1994). The dilution as a function of silica content is a reflection of the compatible nature of transition metals all having a bulk K_D substantially greater than one (Perfit and others, 1999). The decrease in transition metal abundances during fractional crystallization is principally a function of the precipitation of olivine, Fe-Ti oxides, and immiscible sulfides. The crystallization of Fe-Ti oxides is largely governed by the melt redox state. In IAB melts, high pO_2 results in the early crystallization of Fe-Ti oxides and the transitional elements are depleted at an early stage of crystallization. In MORB melts, the low pO_2 results in build up of FeO and TiO_2 in the melt phase during fractional crystallization and the Fe-Ti oxides are a late phase to crystallize. Consequently, the transition metals are depleted at a slower rate in MORB relative to IAB melts.

In principal, the separation of an immiscible sulfide phase should have a dramatic effect on the melt concentrations of transition metals, particularly Ni and Cu. However, sulfur solubility systematics, which control the saturation of sulfides in silicate melts, are complicated by the dissolution of a gaseous sulfur phase. Nonetheless, the systematic behavior of Cu and Zn relative to S suggests that sulfide precipitation is an important process during fractional crystallization in moderating the concentrations of some transition metals. In basalts, the concentrations of S are as high as 1,500 ppm and increase to approx. 2,500 ppm at the andesite stage of crystallization,

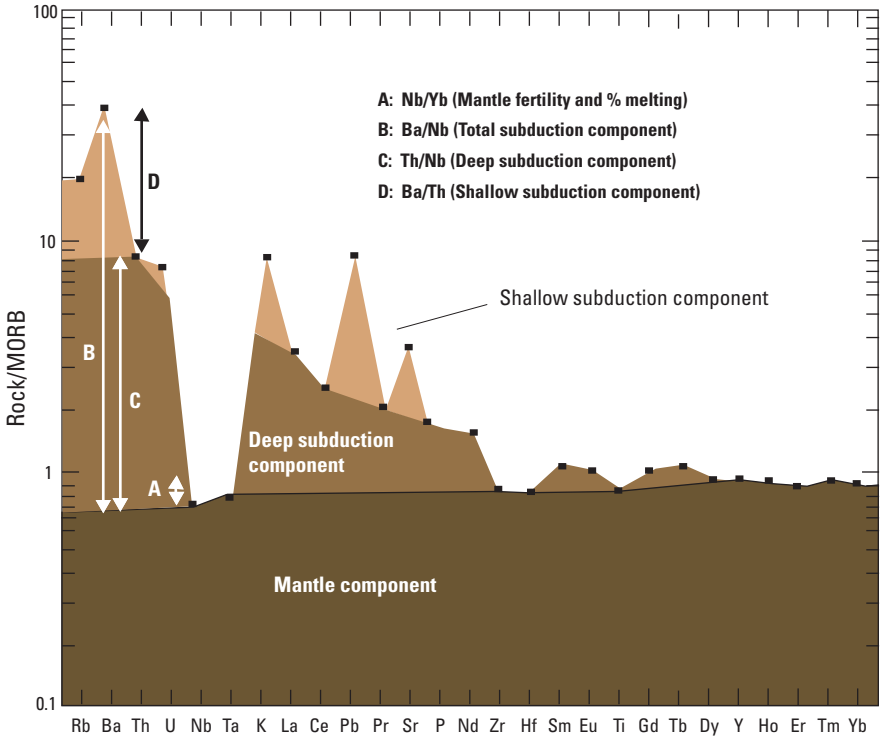

Figure 15–3. The use of trace-element abundances and trace-element ratios as proxies for the subduction input to the overlying mantle preserved in the mantle partial melts that form island-arc and back-arc volcanics. The pristine (depleted) mantle component is represented by mid-ocean ridge basalt (MORB) trace-element values. The deep subduction component is represented by trace-element signatures of partial melting of the subducting crust, that is, concentrations and element ratios that are a function of element incompatibility. The shallow subduction process is represented by trace-element concentrations and ratios that partly reflect sediment-derived fluids. Modified from Pearce and Stern (2006). [Ba, barium; Ce, cerium; Dy, dysprosium; Er, erbium; Eu, europium; Gd, gadolinium; Hf, hafnium; Ho, holmium; K, potassium; La, lanthanum; Nb, niobium; Nd, neodymium; P, phosphorus; Pb, lead; Pr, praseodymium; Rb, rubidium; Sr, strontium; Sm, samarium; Ta, tantalum; Tb, terbium; Th, thorium; Ti, titanium; Tm, thulium; U, uranium; Y, yttrium; Yb, ytterbium; Zr, zirconium]

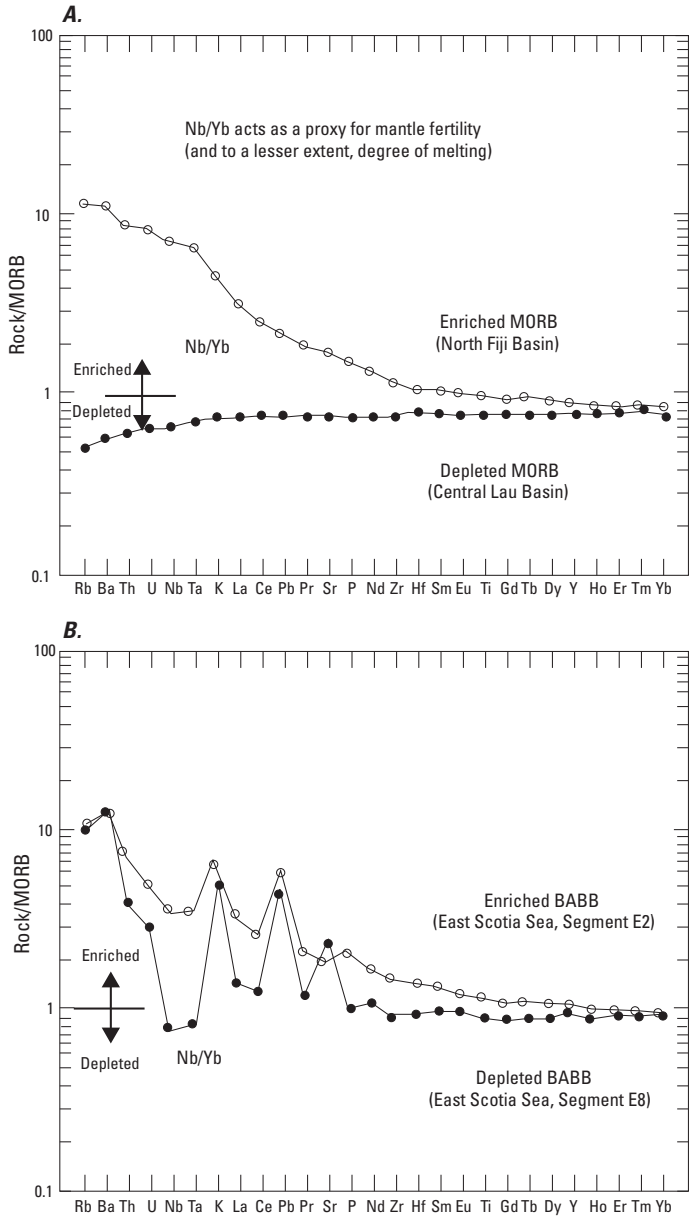

Figure 15–4. Trace-element patterns for several types of volcanics from modern tectonic environments that are commonly associated with volcanogenic massive sulfide (VMS) deposits. These patterns can be compared to those in Piercey (2009) from ancient VMS lithostratigraphic associations. The Nb/Yb ratio is a useful discriminant between enriched and depleted (*A*) mid-ocean ridge basalt (MORB) and (*B*) back-arc basin basalt (BABB). Note that the patterns for BABB are quite distinct from the MORB patterns. The latter reflect degrees of melting of depleted (and perhaps slightly enriched) mantle. The former reflect the additional complexities of subduction dehydration and melting. Modified from Pearce and Stern (2006). [Ba, barium; Ce, cerium; Dy, dysprosium; Er, erbium; Eu, europium; Gd, gadolinium; Hf, hafnium; Ho, holmium; K, potassium; La, lanthanum; Nb, niobium; Nd, neodymium; P, phosphorus; Pb, lead; Pr, praseodymium; Rb, rubidium; Sr, strontium; Sm, samarium; Ta, tantalum; Tb, terbium; Th, thorium; Ti, titanium; Tm, thulium; U, uranium; Y, yttrium; Yb, ytterbium; Zr, zirconium]

after which the abundances steadily decrease. Thus, it is evident that the protoliths to VMS deposits are a rich source of S for hydrothermal fluids.

Isotope Geochemistry

Isotope geochemistry of fresh volcanic rocks is divided into two principal discussions, the radiogenic isotopes (Sr, Nd, Pb) and the stable isotopes. The latter are further divided into the traditional stable isotopes (H, O, S) and the nontraditional isotopes (B, Fe, Cu, Zn). Rubidium and to a lesser degree Sr are alteration mobile elements and may exchange with percolating fluids during hydrothermal alteration (Ridley and others, 1994). Volcanic lithologies associated with VMS deposits may retain some of their isotopic signatures depending upon the degree of alteration, either during hydrothermal flow associated with the formation of VMS deposits or through later metamorphism. It is therefore useful to initially discuss the isotopic signatures of fresh volcanics.

In modern seafloor hydrothermal systems, stable isotopes may be used to examine fluid-flow pathways in exposed stockworks, and this approach also has been used to map paleohydrothermal systems in ancient VMS deposits (Holk and others, 2008).

Radiogenic Isotopes

MORB, OIB, BABB, IAB, and Related Volcanics

Strontium, Neodymium, Lead

Strontium, Nd and Pb isotopic composition of basalts erupted at mid-ocean ridges (Ito and others, 1987) shows a negative correlation between $^{87}Sr/^{86}Sr$ versus $^{143}Nd/^{144}Nd$ and a positive correlation between $^{87}Sr/^{86}Sr$ and Pb isotopes (fig. 15–6).

Probably the most extensively studied of the ocean-based island-arc systems is the Isu-Bonin-Marianas system (Stern and others, 2003). Strontium, Nd and Pb isotopic relationships between IAB volcanics and BABB volcanics are shown in figure 15–7. Back-arc basins include both MORB-type volcanics and back-arc basin volcanics (BABB, *ss*). Although BABB in back-arc basins covers a wide variety of trace-element compositions, the radiogenic and stable isotope compositions are much more restricted and similar to values in MORB from open-ocean settings. BABB volcanics have similar $^{87}Sr/^{86}Sr$ to MORB but have lower $^{143}Nd/^{144}Nd$ and higher values for ^{206}Pb, ^{207}Pb and $^{208}Pb/^{204}Pb$.

Island-arc volcanics carry more radiogenic Sr and Pb and less radiogenic Nd relative to MORB (fig.15–7),

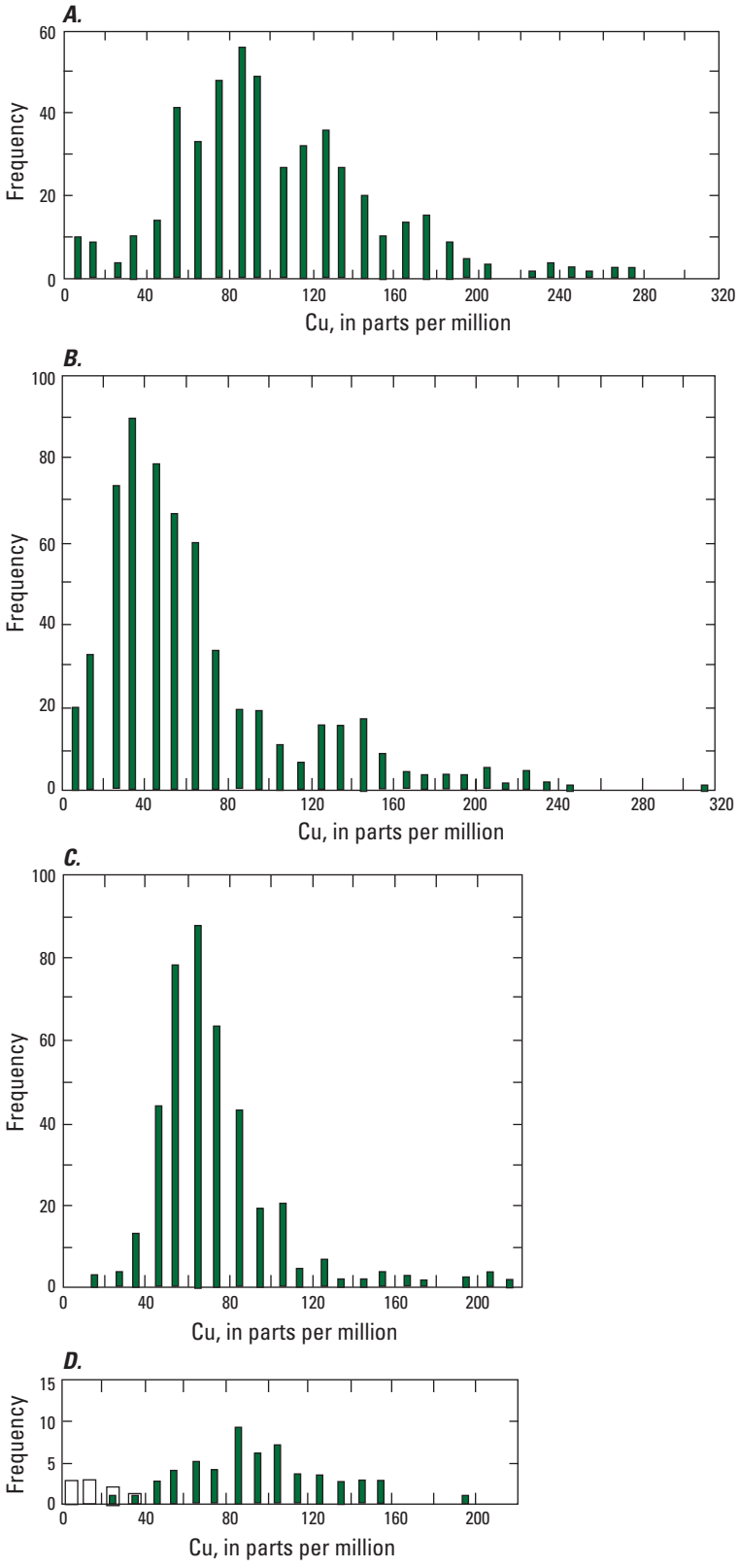

Figure 15–5. Frequency distributions of copper (Cu) in various modern volcanics. *A*, Arc basalts (SiO_2 < 52%). *B*, Arc lavas (SiO_2 > 52%). *C*, Mid-ocean ridge basalt. *D*, Oceanic island basalt (Iceland). Modified from Stanton (1994).

consistent with their higher Rb/Sr ratios and more fractionated REE patterns. These characteristics indicate that the IAB mantle sources are more enriched in lithophile trace elements than the MORB mantle, but also may reflect crustal assimilation and complex crustal mixing processes. This is also consistent with the addition of slab components to the IAB mantle. These components include fluids from dehydration of seawater-altered oceanic crust at shallow subduction levels and partial melts of oceanic crust at deeper levels. Volcanic rocks (andesites, dacites, rhyolites) associated with continental arcs are more radiogenic with regard to Sr, Nd, and Pb compared to island-arc volcanic rocks because of the involvement of highly radiogenic upper continental crust.

Commonly, volcanic rocks show some degree of exchange of Sr with seawater at shallow crustal levels during hydrothermal alteration because seawater contains significant concentrations of Sr (approx. 8 ppm). In modern systems, this is manifest by an overprint of more radiogenic Sr because of the isotopic composition of seawater (0.7091). In ancient VMS deposits, similar alteration processes are likely to occur, except the isotopic composition of seawater is variable in the geologic past (Veizer and others, 1999). In the rock record, if Rb is lost from the system during hydrothermal alteration and exchange with fluids is limited, then the isotopic composition of the original rock may be preserved. However, this is a rare occurrence and most volcanics show Sr exchange with a fluid, either seawater or altered seawater. The latter may have radiogenic Sr inherited from radiogenic continental crust (Whitford and others, 1992). Neodymium isotopes are more robust during hydrothermal alteration because Nd is immobile during alteration, and exchange with seawater is limited by the very low concentrations of Nd in the latter. Lead isotopes are also quite robust; Pb is relatively immobile compared to either U or Th, so the original Pb isotopic composition may be preserved.

Traditional Stable Isotopes

Deuterium/Hydrogen

Because of the large difference in mass between hydrogen and deuterium, D/H fractionations in nature can be very substantial. The hydrogen and oxygen compositions of a variety of waters are shown in figure 15–8.

The hydrogen isotope composition of ancient seawater, based on sediment values, does not appear to have changed much over the past 3 billion years (Sheppard, 1986), and modern ocean water has a canonical value of 0 per mil. Hydrothermal vent

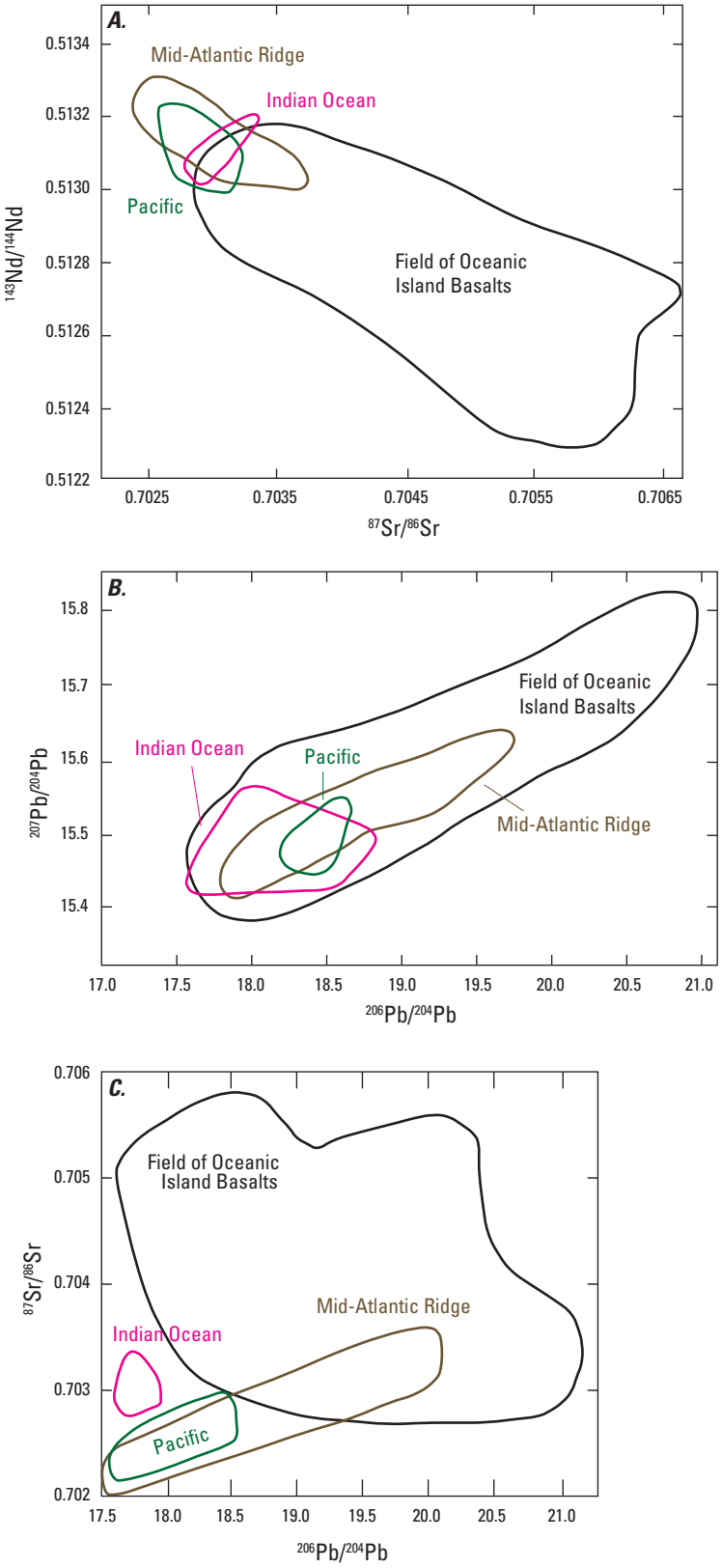

Figure 15–6. Relationships between strontium (Sr), neodymium (Nd), and lead (Pb) isotopes in a variety of mid-ocean ridge basalts (MORB) and oceanic island basalts (OIB). The MORB radiogenic isotopes reflect the nonradiogenic nature of depleted asthenosphere beneath mid-ocean ridges that has been depleted in the Proterozoic. The field of OIB extends to substantially more radiogenic compositions and reflects more radiogenic asthenospheric mantle sources that may have undergone periods of trace-element metasomatism and (or) that include radiogenic plume components. In some cases, the radiogenic OIB also involves a component of lithospheric mantle due to lithospheric thining above an ascending plume head.

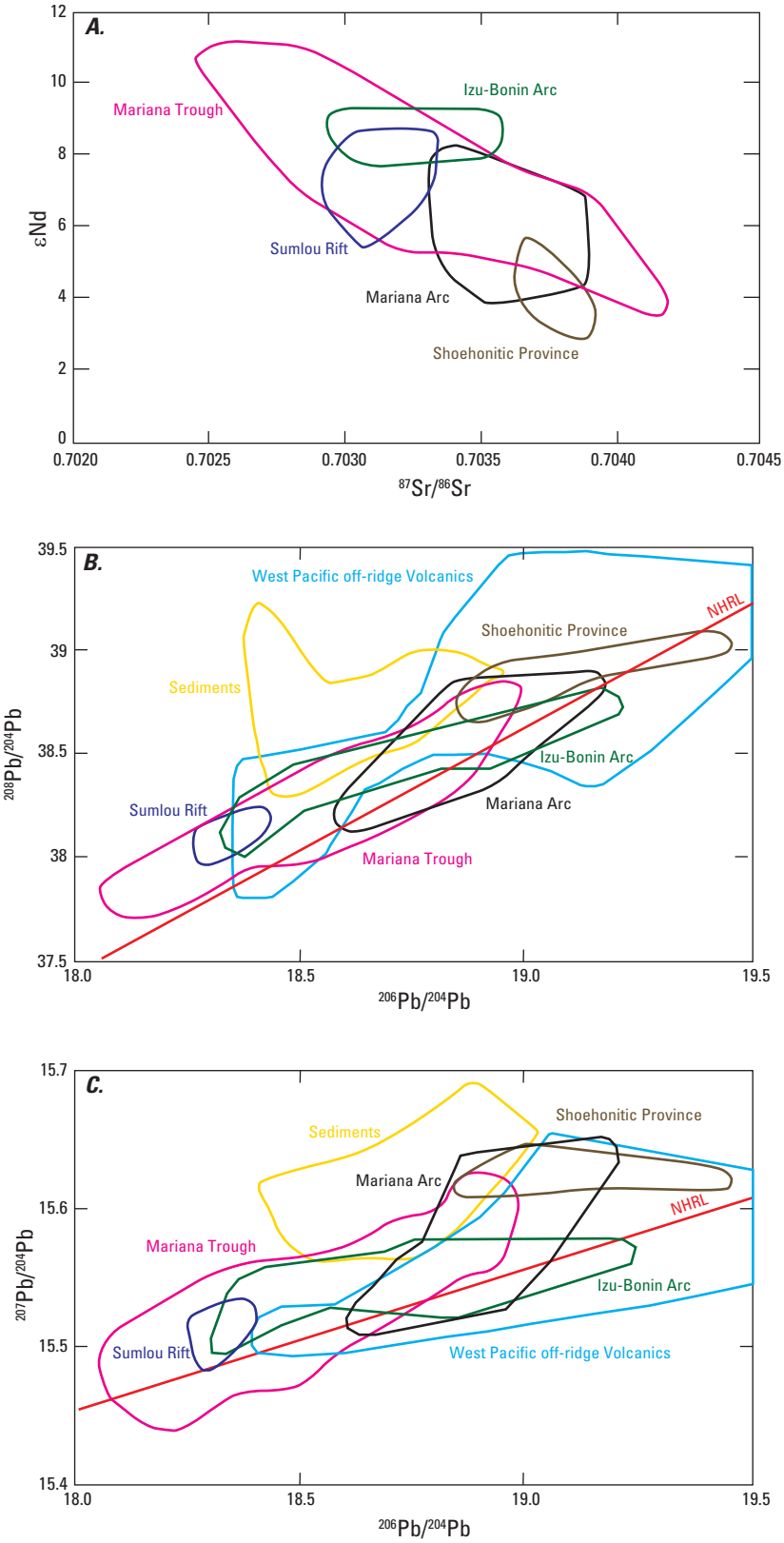

Figure 15–7. Strontium (Sr), neodymium (Nd), and lead (Pb) isotopic variability in island-arc basalt (IAB) volcanics (Izu-Bonin, Marianas arcs, shoshonite province) and back-arc basin basalt (BABB) volcanics (Mariana Trough). The majority of the BABB volcanics have Sr isotope values <0.7032 and εNd values >9 and, thus, are distinct from most IAB volcanics, but similar to mid-ocean ridge basalt (MORB). The IAB volcanics are uniformly more radiogenic than MORB but overlap the field of OIBs. The field of shoshonite volcanics (late-stage IAB volcanism) has the most radiogenic Sr compositions. Although it is reasonable to assume that the radiogenic isotope composition of IAB volcanics reflects variable input of radiogenic isotopes from the subducting slab, the data alone cannot preclude the possibility that the IAB and OIB mantles are similar. [NHRL, Northern Hemisphere Reference Line]

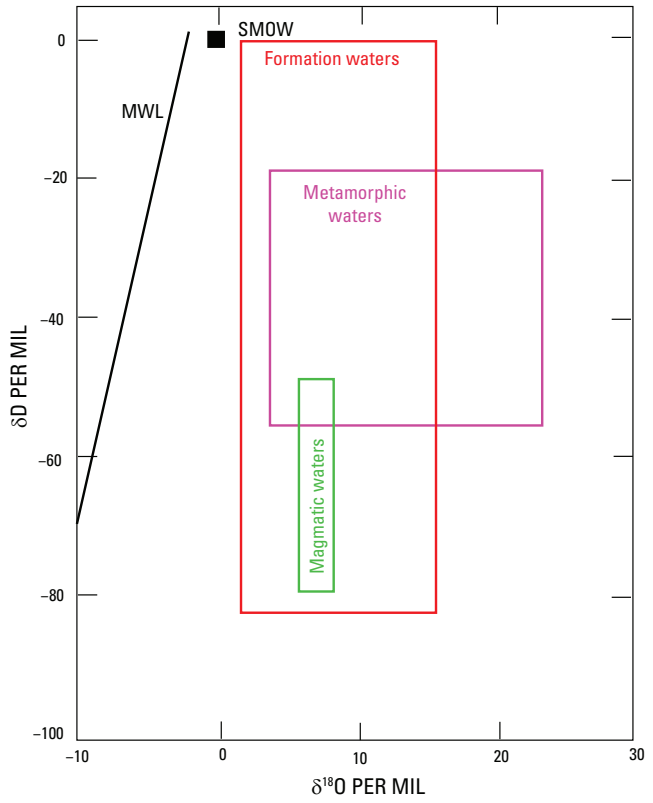

Figure 15–8. Hydrogen and oxygen isotopic composition of various types of terrestrial waters. Modified from Hoefs (2004). [SMOW, standard mean ocean water; MWL, meteoric water line]

fluids have δD values close to seawater (3 to -2 per mil) as a result of fluid/rock reactions under variable water/rock ratios, phase separation in some cases, and addition of small amounts of magmatic water (Shanks and others, 1995). Most magmatic waters have δD values between -50 and -85 per mil, within the range found in MORB and OIB volcanics. Magmatic waters associated with mafic magmas range from -60 to -80 per mil, whereas those associated with felsic magmas range from -85 to -18 per mil. Oceanic basalts (MORB and OIB) show a range in δD values from -20 to -100 per mil with an average value of -80 per mil (Bell and Ihinger, 2000, and references therein). A part of this variation may result from loss of hydrogen during eruption by outgassing of H_2O and, in limited cases, outgassing of CH_4 and H_2, which all cause isotopic fractionation. Kyser and O'Neil (1984) and Poreda and others (1986) suggest that the primary δD values for MORB and OIB volcanics are indistinguishable at -80±5 per mil, similar to values for continental lithosphere (-63 to -70 for phlogopites in kimberlites; Boettcher and O'Neal, 1980). This value is distinct from the values observed in hydrous mantle minerals (-20 to -140 per mil) and in nominally anhydrous mantle minerals (-90 to -120 per mil). These large ranges in δD values suggest either perturbation of the "mantle value" by interactions with surface and near-surface fluids and (or) an upper mantle that is heterogeneous with regard to hydrogen isotopic composition.

Back-arc basin basalts have been measured from Lau Basin and Mariana Trough (Poreda, 1985) and from Okinawa Trough (Honma and others, 1991). The Lau samples and Okinawa Trough samples have δD values that are MORB-like (-63 to -70 per mil) and do not require a mantle source with a subduction-related component. This is consistent with other radiogenic isotope and trace element data that indicate MORB-type mantle beneath the Lau Basin. In contrast, BABB samples from the Mariana Trough and Okinawa Trough are isotopically heavier (Mariana: -32 to -46 per mil; Okinawa: -50 per mil), indicating a mantle component of water (about -25 per mil) from the subducting slab.

Crystal fractionation in magmatic systems extends the range of hydrogen isotope compositions to lighter values, and δD values of -140 have been measured in rhyolites that have magmatic $\delta^{18}O$ values and thus have not been contaminated by assimilation of meteoric water. Frequently, the hydrogen isotope composition is correlated with water content; δD decreases with decreasing wt% H_2O, suggesting that the range of isotopic compositions is related to magmatic degassing.

Deep drilling in the modern oceans provides a perspective on the changes in hydrogen isotopic composition of altered oceanic crust caused by deep hydrothermal circulation. The 2.5-km-deep core from ODP Hole 504B shows that the pillow basalts of Layer 2A have variable δD values (-60 to -110 per mil), whereas the sheeted dike section of Layer 2B has more uniform δD values (about -40 per mil) (Alt and others, 1996). The latter values are consistent with exchange of hydrogen between evolved seawater (1–2 per mil) and pristine volcanics at high temperatures (350 °C to >400 °C), whereas the variability of the former reflect fluid/rock reactions between altered seawater, pristine seawater, and volcanics at a range of lower temperatures (Shanks, 2001).

Huston (1999) provides a synopsis of D/H data for ore fluids associated with VMS deposits. Table 15–5 incorporates these data with temperature information from fluid/mineral $\delta^{18}O$ equilibria. Table 15–5 also provides information on δD values for whole rocks and minerals. A general consensus of this information, when combined with $\delta^{18}O$, is that the ore-forming fluids for VMS deposits and rock alteration fluids have seawater or altered seawater compositions and circulated at a wide variety of temperatures from <125 °C to >350 °C. In some deposits there is an increase in δD toward ore and increasing grade of alteration (West Shasta, Troodos, some Kuroko deposits) but at others (Ducktown, Kidd Creek) postmineralization/postalteration metamorphism has acted to homogenize δD (Huston, 1999).

$^{18}O/^{16}O$

A useful overview of the oxygen isotopic composition of volcanic rocks is provided by Eiler (2001). The oxygen isotope composition (expressed in $\delta^{18}O$ notation) of fresh MORB is almost invariant at 5–6 per mil (Eiler, 2001). This

Table 15–5. Hydrogen isotope compositions of ore and alteration fluids, whole rocks, and minerals for selected volcanogenic massive sulfide deposits. Modified from Huston (1999), with additions.

[D, deuterium; O, oxygen; T, temperature]

District/ deposit	Association	Temperature (°C)	δD (mineral)	δD (rock)	δD (fluid)	$\delta^{18}O$ (fluid)	Comment	Reference
Modern seafloor	mafic	200–410 °C		–60 to –120	1 ± 3	0.4 to 2.1	Layer 2A lavas	Shanks (2001)
				–20 to –60			Layer 2B dikes	
Kuroko-type	siliciclasic-felsic							
Hokuroku, Japan		230–270			–10 to –30	–2.3 to 0.9	Fluid inclusion analysis	Ohmoto and Rye (1974); Hattori and Sakai (1979)
Kosaka, Japan		220–230			15 to –30	–1.0 to 3.0	Fluid inclusion analysis	Hattori and Muehlenbachs (1980); Pisutha-Armond and Ohmoto (1983)
Iwami, Japan		230–270			–35 to –55	–3.4 to –1.6	Fluid inclusion analysis	Hattori and Sakai (1979)
Inarizami, Japan			–24 to –32				Kaolin minerals	Marumo (1989)
Minamishiraoi, Japan							Kaolin minerals	Marumo (1989)
Troodos, Cyprus	mafic	~ 350		–43 to –78 (least altered); –33 to –41 (altered)	5 to –5	–0.5 to 1.5	Assumed temperature	Heaton and Sheppard (1977)
Josephine, USA	mafic	150–250		–38 to –54	0 to –7		$\delta^{18}O$ mineral-fluid equilibria for T	Harper and others (1988)
		250–450		–37 to –50	0 to –7		$\delta^{18}O$ mineral-fluid equilibria for T	
		450–600		–45 to –59	0 to –7		$\delta^{18}O$ mineral-fluid equilibria for T	
		>600		–35	0 to –7		$\delta^{18}O$ mineral-fluid equilibria for T	
Buchans, Canada		240–370			–6 to –10	–1.5 to 4.5	$\delta^{18}O$ mineral-fluid equilibria for T	Kowalik and others (1981)
Iberian Pyrite Belt	siliciclastic-felsic							
Aljustrel		200–270 (stockwork)	–32 to –40 (chlorite)		0 to 15	1.3 to 5.1	$\delta^{18}O$ mineral-fluid equilibria for T	Munha and others (1986)
		160–175 (ore zone)			0 to 15		$\delta^{18}O$ mineral-fluid equilibria for T	
		120 (hanging wall)			0 to 15		$\delta^{18}O$ mineral-fluid equilibria for T	

Table 15–5. Hydrogen isotope compositions of ore and alteration fluids, whole rocks, and minerals for selected volcanogenic massive sulfide deposits. Modified from Huston (1999), with additions.—Continued

[D, deuterium; O, oxygen; T, temperature]

District/ deposit	Association	Temperature (°C)	δD (mineral)	δD (rock)	δD (fluid)	δ18O (fluid)	Comment	Reference
Feitas-Estação		200–270 (stockwork)	–32 to –40 (chlorite)		0 to 15		$\delta^{18}O$ mineral-fluid equilibria for T	Munha and others (1986)
		160–175 (ore zone)			0 to 15		$\delta^{18}O$ mineral-fluid equilibria for T	
		120 (hanging wall)			0 to 15		$\delta^{18}O$ mineral-fluid equilibria for T	
Rio Tinto		210–230	–40 to –45 (chlorite)		–5 to +8	0 to 1.4	$\delta^{18}O$ mineral-fluid equilibria for T	Munha and others (1986)
Chanca		220	–40 to –45 (chlorite)		–10 to 0	0.9	$\delta^{18}O$ mineral-fluid equilibria for T	Munha and others (1986)
Salgadinho		230	–30 (muscovite)		–10 to 0	4.0	$\delta^{18}O$ mineral-fluid equilibria for T	Munha and others (1986)
Crandon, USA	siliciclastic-felsic	210–290		–50 to –52 (distal footwall)	–2 to –12	–1.7 to –0.1		Munha and others (1986)
				–55 (footwall)				
				–50 to –52 (hanging wall)				
West Shasta, USA	siliciclastic-felsic	200–300		–45 to –73 (basalt to dacite)	0 (assumed)		Assumed temperature	Casey and Taylor (1982); Taylor and South (1985)
				–50 to –65 (trond-hjemite)				
Blue Hill, USA	bimodal-mafic	240–350	–54 to –65(mus-covite),					
–60 to –68 (chlorite)		–20 to –38	5.0 to 7.0	$\delta^{18}O$ mineral-fluid equilibria for T	Munha and others (1986)			

Table 15–5. Hydrogen isotope compositions of ore and alteration fluids, whole rocks, and minerals for selected volcanogenic massive sulfide deposits. Modified from Huston (1999), with additions.—Continued

[D, deuterium; O, oxygen; T, temperature]

District/ deposit	Association	Temperature (°C)	δD (mineral)	δD (rock)	δD (fluid)	δ18O (fluid)	Comment	Reference
Ducktown, USA	siliciclastic-felsic	450–580	–69 to –76 (country rock biotite); –59 to –50 (country rock muscovite); –68 to –77 (ore zone biotite); –51 to –54 (ore zone muscovite); –62 to –69 (ore zone chlorite)		–33 to –36 (local alteration), –31 to –32 (regional)	5.4 to 7.0	$\delta^{18}O$ mineral-fluid equilibria for T	Addy and Ypma (1977)
Bruce, USA	siliciclastic-felsic	250–300				1.1 to 2.1	Assumed temperature	Larson (1984)
Mattgami Lake, Canada	bimodalmafic	240–350			0.5 to 2.0		Fluid inclusions; mineral equilibria	Costa and others (1983)
Noranda								
Horne	bimodal-mafic	250–350			–30 to –40	1.5 to 4.5	$\delta^{18}O$ mineral-fluid equilibria for T	MacLean and Hoy (1991); Hoy (1993)
Mobrun	bimodal-mafic	150–250				0 to 4.0	$\delta^{18}O$ mineral-fluid equilibria for T	Hoy (1993)
Norbec	bimodal-mafic	200–300				–1.0 to 3.0	$\delta^{18}O$ mineral-fluid equilibria for T	Hoy (1993)
Amulet	bimodal-mafic	250–350				–0.5 to 2.0	$\delta^{18}O$ mineral-fluid equilibria for T	Hoy (1993)
Ansil	bimodal-mafic	200–350				–2.0 to 1.0	$\delta^{18}O$ mineral-fluid equilibria for T	Hoy (1993)
Corbet	bimodal-mafic	250–300				–4.0 to 0		Hoy (1993)

Table 15–5. Hydrogen isotope compositions of ore and alteration fluids, whole rocks, and minerals for selected volcanogenic massive sulfide deposits. Modified from Huston (1999), with additions.—Continued

[D, deuterium; O, oxygen; T, temperature]

District/ deposit	Association	Temperature (°C)	δD (mineral)	δD (rock)	δD (fluid)	δ18O (fluid)	Comment	Reference
Kidd Creek, Canada	bimodal-mafic	300–350		Local				Huston and Taylor (1999)
				–25 to –50 (qz porphyry)	–13 to –3	3.3 to 4.3	$\delta^{18}O$ mineral-fluid equilibria for T	
				–25 to –70 (ore host rhyolite)				
				–25 to –70 (footwall rhyolite)				
				Regional				Taylor and Huston (1999)
				–25 to –60 (mafics)	+20	4	$\delta^{18}O$ mineral-fluid equilibria for T	
				–25 to –65 (ultramafics				
				–15 to –45 (felsics)				
South Bay, Canada	bimodal-felsic	300				2.1 to 4.5	$\delta^{18}O$ mineral-fluid equilibria for T	Urabe and Scott (1983)

is also the value for fresh mantle peridotites, so is assumed to be the mantle value. Ito and others (1987) could not find isotopic variations related to geographic setting or MORB type (DMORB to EMORB). However, high precision oxygen isotope data (Eiler and others, 2000) reveal subtle variations that systematically relate to incompatible element concentrations and ratios and are interpreted in terms of fractional crystallization and subtle variations in the isotopic composition of mantle sources. Ocean-island basalt shows a slightly extended range of oxygen isotope values (4.6–6.1 per mil) compared to MORB samples, which reflect the more complex mantle source reservoirs of OIB. Lower isotopic values may reflect the involvement of ancient lower oceanic crust whereas higher values may reflect a component of pelagic sediment (fig. 15–8).

Back-arc basin basalt shows a relatively restricted range of oxygen isotope compositions. Sixteen basalts from the Lau Basin vary between 5.6 and 6.4 per mil, and seven basalts from the Mariana Trough vary from 5.5 to 5.7 per mil. Island-arc basalts and related volcanics show a wider range of oxygen isotope compositions compared to MORB, OIB, or BABB volcanics. In IAB mafic volcanics, the range is small (4.8–5.8 per mil) but is larger if more evolved felsic volcanics are included, as high as 14 per mil. Only part of this variation can be related to crystal fractionation, which is expected to increase the isotopic composition by only about 1–2 per mil. The $\delta^{18}O$ values of IAB magmas and their derivatives are complicated by the potential for mixing and assimilation if magma erupts through thick sequences of sediment and (or) continental crust. The higher $\delta^{18}O$ values for IABs, relative to MORB, almost certainly reflect some type of contamination, probably from pelagic sediment. Recent measurements (Eiler, 2001) suggest that the range of uncontaminated volcanics is 5±1 per mil, identical to the MORB values, but that there may be subtle indications of the effects of material added to the mantle from the subducted slab.

In modern seafloor hydrothermal systems, perturbation of the pristine oxygen isotope compositions of volcanics occurs by alteration of the oceanic crust by seawater ($\delta^{18}O$ = 0 per mil) or evolved seawater, that is, vent fluids ($\delta^{18}O$ = 0.5–2 per mil), a process that is a function of depth (a proxy for temperature) and spreading rate. The oxygen isotopic composition of seawater is perturbed because of water/rock reactions that cause isotopic exchange between circulating fluids and primary minerals, resulting in isotopic equilibria between fluid and secondary minerals (Shanks, 2001).

At intermediate- and slow-spreading ridges, the tectonic disruption of the oceanic crust results in increased permeability and fracture porosity, allowing for deep penetration of seawater, cooling of the crust and alteration assemblages formed at low temperatures. Under these circumstances, the overall fluid pathway is increased in length, allowing for greater extents of fluid/rock interaction (Bach and Humphris, 1999). At fast-spreading ridges, the crustal structure is less tectonically disturbed, and lower porosity and permeability allow circulating fluids to maintain higher temperatures (Alt and Teagle, 2003). At slow-spreading ridges such as the Costa Rica rift (spreading rate 5 cm/yr), the hydrothermal circulation extends to the base of Layer 2B (sheeted dike complex) where depleted oxygen isotope compositions, as low as 4 per mil (Alt and others, 1996; Shanks, 2001), are observed. Hydrothermal fluids that penetrate into the upper homogeneous gabbros of Layer 3 also show a range of $\delta^{18}O$ values from 2 to 7.5 per mil (Shanks, 2001). In the upper parts of Layer 2B, enriched oxygen isotope compositions are observed, 8 per mil or higher, and elevated values are found in Layer 2A (fig. 15–9).

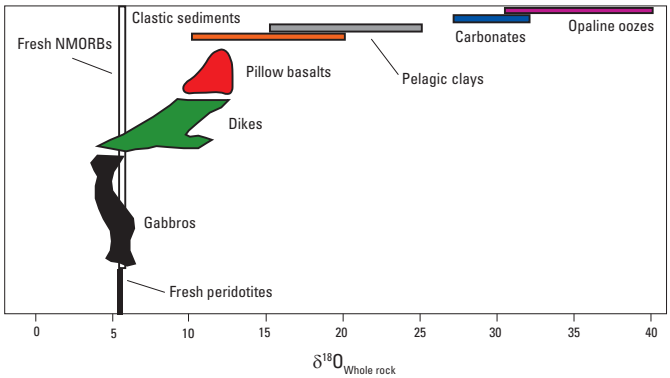

Figure 15–9. Oxygen isotopic composition of various lithologic units relative to mid-ocean ridge basalt (MORB). The sequence of peridotite–gabbro–dikes–pillow basalts represents a sequence through oceanic crust typically observed in ophiolites. The isotopic variability in this sequence reflects hydrothermal exchange with hydrothermal fluids and seawater. Modified from Eiler (2001).

Taylor (1974) demonstrated the utility of oxygen isotopes in ore deposit studies and Heaton and Sheppard (1977) first demonstrated, at Troodos, systematic variations in $\delta^{18}O$ of volcanic rocks hosting VMS deposits. Taylor (1990) recognized three types of fossil hydrothermal systems, based on temporal factors, temperatures, and water/rock ratios. Although applicable to a wide range of ore deposits, from epithermal to mesothermal, the classification does have relevance to VMS deposits. The three types, which are not mutually exclusive in space and time, are (Hoefs, 2004):

- Type I—Epizonal systems with a variety of $\delta^{18}O$ values and extreme isotopic disequilibria between coexisting mineral phases. These systems have temperatures between 200 and 600 °C and lifetimes of $<10^6$ years. Type I systems are most applicable to VMS systems that form at <3–4 km depth and involve the totality of hydrothermal flow from surface to the proximal parts of subsurface intrusions.

- Type II—Deeper-seated and (or) longer lived systems, also with a range of whole-rock $\delta^{18}O$ values but with equilibrium between coexisting mineral phases. These systems have temperatures between 400 and 700 °C

and life times of >10^6 years. Some of the deeper parts of large VMS systems may be included in this category.

- Type III—Equilibrated systems with uniform $\delta^{18}O$ in all lithologies. These systems require large water/rock ratios and high temperatures (500–800 °C) and long life times (about 5×10^6 years).

Subsequent to these studies, there have been many studies that deal with various aspects of oxygen isotope variability in volcanic rocks that host VMS deposits (table 15–6). Volcanics associated with VMS deposits invariably show some degree of exchange of oxygen during hydrothermal alteration. Wherever detailed studies have been performed, the isotopic composition of altered volcanics can be correlated with specific zones of alteration that may be conformable or crosscut local and regional lithologies. These correlations are a function of alteration temperatures and fluid/rock ratios that produce alteration zones from zeolite facies through upper greenschist facies. In some cases, these alteration zones may be overprinted by later amphibolite facies assemblages. In many cases, these fluid systems are of regional extent, extending laterally for several kilometers outside of the immediate domains of ore deposits. They also may extend vertically for hundreds of meters into the footwall lithologies and into hanging wall lithologies. Table 15–7 provides a synopsis of the range of $\delta^{18}O$ values observed in volcanic rocks associated with VMS deposits.

$\delta^{34}S$

The mantle value for $\delta^{34}S$ varies from -7 to 7 per mil. High-S peridotites have values from about 0 to -5 per mil, whereas low-S peridotites have values from about 0 to +5 per mil (Ionov and others, 1992). Most fresh MORB samples have $\delta^{34}S$ values of 0±2 per mil (Sakai and others, 1984). However, hydrothermally altered MORB has significantly heavier $\delta^{34}S$ values that generally correlate with $^{87}Sr/^{86}Sr$ because of interaction with modern seawater ($\delta^{34}S$ approx. 21 per mil). The principal sulfur gas in equilibrium with mafic melts at low pressure and high temperature is SO_2. With decreasing temperature and (or) increasing fH_2O, H_2S becomes more stable. Modern volcanic gases associated with basaltic volcanism have $\delta^{34}S$ of about 1±1.5 per mil (Sakai and others, 1982; Allard, 1983), whereas gases associated with felsic volcanism have heavier $\delta^{34}S$ values (up to 5 per mil; Poorter and others, 1991).

Alteration of volcanics associated with VMS deposits results in changes in bulk $\delta^{34}S$ due to precipitation of sulfide and (or) sulfate minerals.

Depth of Emplacement

The location of heat that drives hydrothermal circulation is uncertain in most modern VMS settings. In ancient VMS settings, a systematic relationship between hydrothermal alteration and the location of a specific intrusive body may also provide depth information, but the common dismemberment of VMS deposits makes this criterion difficult to apply. In modern MOR settings, small melt lenses have been seismically imaged beneath several segments of the East Pacific Rise, along the Juan de Fuca Ridge, and at the Mid-Atlantic Ridge. The melt lenses frequently are associated with surface hydrothermal venting. They are assumed to be the heat source that drives the hydrothermal circulation and lie close to the base of Layer 2B that is at approximately 2 km beneath the ocean floor at fast spreading ridges (Singh and others, 1999) and up to 3 km at slow spreading ridges (Sinha and others, 1998). These depths are expected to be appropriate for VMS deposits with mafic-ultramafic volcanic associations. However, at MOR and back-arc settings, the high-level melt lenses are underlain with a substantial (several kilometers) crystal-melt mush that also must contribute to the thermal energy required to drive hydrothermal circulation. The common association of VMS deposits with felsic volcanics, even in mafic-dominated environments, suggests that felsic plutons provided the required heat. The presence of felsic volcanics at the surface presumably implies the presence of felsic intrusions at depth, although little is known as to the exact depth. Generally, in modern environments, individual high-level intrusions are ephemeral in their ability to supply heat to drive hydrothermal circulation.

Table 15–6. Selected oxygen isotope studies of volcanic rocks hosting volcanogenic massive sulfide (VMS) deposits.

Deposit	Age	Application	Reference
General		Taylor: Seminal study of δ18O variations in lithostratigraphic successions associated with a wide variety of ore deposits, including VMS deposits of western Cascades. Huston: An in-depth review of stable isotope geochemistry applied to VMS deposits	Taylor (1974); Huston (1999)
Kidd Creek, Ontario	Archean	Isotope composition of hanging wall and footwall rhyolites and mafic volcanics (bimodal mafic association). Regional isotope mapping recognizes isotopic shifts due to hydrothermal alteration and regional greenschist facies metamorphism.	Beaty and others (1988); Huston and others (1995); Huston and Taylor (1999)
Sturgeon Lake, Ontario	Archean	Local and regional scale isotope studies of caldera complex (bimodal felsic association). Identified syn- and post-mineralization fluids of hydrothermal (modified seawater) and seawater origin and fluid temperatures.	King and others (2000); Holk and others (2008)
Noranda, Quebec	Archean	Local and regional scale isotope mapping of volcanic sequences (bimodal mafic association) to understand fluid flow and nature of hydrothermal fluids.	Beaty and Taylor (1982); Cathles (1993); Hoy (1993); Paradis and others (1993)
Mattagami Lake, Quebec	Archean	Origin of hydrothermal fluids in shallow brine pool	Costa and others (1983)
Hercules, Tasmania	Cambrian	Use of stable isotopes for regional exploration	Green and Taheri (1992)
Samail, Oman	Cretaceous	Regional isotope study of classical "Penrose" ophiolite (mafic association). Pillow lavas and sheeted dikes are isotopically enriched, gabbros and peridotites are depleted due to interactions with seawater at shallow levels and altered seawater at deeper levels. Hydrothermal fluids penetrated to Moho in off-axis sections	Gregory and Taylor (1981); Stakes and Taylor (1992)
Josephine, United States	Jurassic	Regional study of ophiolite complex, mainly extrusive sequence and sheeted dikes (mafic association). Isotopic compositions allow recognition of discharge and recharge zones	Harper and others (1988)
West Shasta, United States	Devonian	Regional scale study of mining district (siliciclastc felsic association) to identify fluid sources and temperatures of alteration.	Casey and Taylor (1982); Taylor and South (1985)
Iberian Pyrite Belt, Spain and Portugal	Carboniferous	Regional isotopic study (siliciclastic-felsic associ tion) to understand nature of ore fluids, some being basinal brines.	Munha and Kerrich (1980); Munha and others (1986); Tornos and others (2008)
Crandon, United States	Proterozoic	Local and regional isotope study to evaluate fluid compositions and temperatures.	Munha and others (1986)
Kuroko, Japan	Miocene	Regional (district-wide)and local (mine scale) studies of lithostratigraphic units (siliciclastic-felsic association) to identify isotopic variations as function of alteration grade and establish exploration strategies.	Ohmoto and Rye (1974); Green and others (1983); Pisutha-Arnond and Rye (1983); Watanabe and Sakai (1983); Marumo (1989)

Table 15–7. Whole rock $\delta^{18}O$ values for lithostratigraphic units associated with volcanogenic massive sulfide deposits (selected studies). Modified from Huston (1999), with additions.

[O, oxygen; alb, albite; amph, amphibole; carb, carbonate; chl, chlorite; epi, epidote; fuch, fuchsite; kaol, kaolinite; mont, montmarillonite; qz, quartz; ser, sericite; sil, sillimanite; zeol, zeolite]

Deposit	Association	Age	$\delta^{18}O$ (least altered lithologies)	$\delta^{18}O$ (most altered lithologies)	Alteration zones/ lithology	References
Fukazawa, Japan	Siliciclastic-felsic	Miocene	11.6–22.4		zeol	Green and others (1983)
			6.5–16.8		mont	
				4.6–10.5	ser-chl	
Uwamuki, Japan	Siliciclastic-felsic	Miocene	8.8–10.4		kaol-qz-ser±chl±alb	Urabe and others (1983)
			7.3–10.9		alb-ser-chl-qz	Hattori and Muehlenbachs (1980)
				8.2–9.6	clay-ser-chl-qz (1980)	
				7.0–9.2	ser-chl-qz	
				6.7–8.6	qz-ser	
				8.1–8.3	sil	
Troodos, Cyprus	Mafic	Cretaceous	11.8–16.0		Upper pillow lavas	
				1.4–4.1	Stockwork	
Samail, Oman	Mafic	Cretaceous		2.0–7.0	Gabbro	Stakes and Taylor (1992)
				5.0–9.0	epi-chl sheeted dikes	
				6.0–9.0	epi-chl pillow lavas	
Seneca, Canada		Jurassic	10.7–11.6		Felsic breccia	Urabe and others (1983)
				6.9–8.7	Sil felsic breccia	
Freitas-Estação, Portugal	Siliciclastic-felsic	Carboniferous	15.7–18.1		Volcanoclastic rhyolites	Barriga and Kerrich (1984)
				13.9–14.4	Stockwork-peripheral	
				11.6–12.5	Stockwork	
Hercules, Tasmania	Siliciclastic-felsic	Cambrian	11.2–15.5		Rhyolitic flows	Green and Taheri (1992)
				6.8–10.0	qz-chl-ser	
Hellyer, Tasmania	Siliciclastic-felsic	Cambrian	10.4–12.2		Footwall andesite	Green and Teheri (1992)
				8.0–11.6	ser-qz stringer (distal)	
				7.0–9.6	chl-ser stringer (proximal)	
			9.6–14.0		Hanging wall basalt	
				9.4–11.8	fuch-carb hanging wall basalt	
Ducktown, United States	Siliciclastic-felsic?	Proterozoic	8.6–10.8		Country rock	Addy and Ypma (1977)
			10.2–11.5		qz (counrty rock)	
				8.3–9.7	qz (altered rock)	
				8.1–10.3	qz (ore zone)	

Table 15–7. Whole rock $\delta^{18}O$ values for lithostratigraphic units associated with volcanogenic massive sulfide deposits (selected studies). Modified from Huston (1999), with additions.—Continued

[O, oxygen; alb, albite; amph, amphibole; carb, carbonate; chl, chlorite; epi, epidote; fuch, fuchsite; kaol, kaolinite; mont, montmarillonite; qz, quartz; ser, sericite; sil, sillimanite; zeol, zeolite]

Deposit	Association	Age	$\delta^{18}O$ (least altered lithologies)	$\delta^{18}O$ (most altered lithologies)	Alteration zones/ lithology	References
Bruce, United States	Siliciclastic-felsic	Proterozoic	6.0–7.6		andesite	
				2.4–5.6	chl	
Mattagami Lake, Canada	Bimodal-mafic	Archean	8.5–9.2		rhyolite	Costa and others (1983)
				2.0–7.6	rhyolite	
				1.8–4.9	chl altered footwall	
Horne, Canada	Bimodal-mafic	Archean	7.0–9.0		rhyolite	Hoy (1993)
				6.6–11.6	qz-ser-chl rhyolite	
				3.9–4.4	chl-rich rhyolite	
Mobrun, Canada	Bimodal-mafic	Archean	6.0–14.0		qz-ser rhyolite	Hoy (1993)
Norbec, Canada	Bimodal-mafic	Archean		3.0–7.0	dalm below ore	Hoy (1993)
					qz-ser rhyolite	
Amulet, Canada	Bimodal-mafic	Archean	6.3–6.4		andesite	Beaty and Taylor (1982)
				4.0–4.8	grid fractured zone (stock-work?)	
				3.6–3.8	dalm	
Ansil, Canada	Bimodal-mafic	Archean	4.0–6.0		rhyolite, andesite	Hoy (1993)
				2.0–4.0	qz-ser altered rhyolite, andesite	
Corbet, Canada	Bimodal-mafic	Archean	6.0–9.8		andesite	Urabe and others (1983)
				2.3–4.2	ore zone	
Kidd Creek, Canada	Bimodal-mafic	Archean	12.0–15.8		rhyolite	Beaty and others (1988)
			9.7–14.9		rhyolite (ore host)	Huston and Taylor (1999); Beaty and others (1988)
			9.1–13.6		hanging wall porphyry	Huston and Taylor (1999)
				9.0–12.3	cherty breccia	
				4.3–7.8	chloritite	

Table 15–7. Whole rock $\delta^{18}O$ values for lithostratigraphic units associated with volcanogenic massive sulfide deposits (selected studies). Modified from Huston (1999), with additions.—Continued

[O, oxygen; alb, albite; amph, amphibole; carb, carbonate; chl, chlorite; epi, epidote; fuch, fuchsite; kaol, kaolinite; mont, montmarillonite; qz, quartz; ser, sericite; sil, sillimanite; zeol, zeolite]

Deposit	Association	Age	$\delta^{18}O$ (least altered lithologies)	$\delta^{18}O$ (most altered lithologies)	Alteration zones/ lithology	References
Sturgeon Lake, Canada	Bimodal-felsic	Archean	7.2–7.9		gabbro, tonalite	King and others (2000);
				7.0–7.4	chl-epi-amph (intrusives)	Holk and others (2008)
				12.3–14.3	epi-chl-ser	
				9.00–15.0	sil	
				8.34–13.3	rhyolite (ore host)	
				11.05–14.3	andesite	

References Cited

Addy, S.K., and Ypma, P.J.M., 1977, Origin of massive sulfide deposits at Ducktown, Tennessee—An oxygen, carbon, and hydrogen isotope study: Economic Geology, v. 72, p. 1245–1268.

Allard, P., 1983, The origin of hydrogen, carbon, sulphur, nitrogen, and rare gases in volcanic exhalatives—Evidence from isotope geochemistry, *in* Tazieff, H., and Sabroux, J.C., eds., Forecasting volcanic events: Amsterdam, Elsevier, p. 233–246.

Allen, D.E., and Seyfried, W.E., Jr., 2004, Serpentinization and heat generation—Constraints from Lost City and Rainbow hydrothermal systems: Geochimica et Cosmochimica Acta, v. 68, no. 6, p. 1347–1354.

Alt, J.C., Laverne, C., Vanko, D., Tartarotti, P., Teagle, D.A.H., Bach, W., Zuleger, E., Erzinger, J., Honnerez, J., Pezard, P.A., Becker, K., Salisbury, M.H., and Wilkens, R.H., 1996, Hydrothermal alteration of a section of upper oceanic crust in the eastern equatorial Pacific, *in* Alt, J.C., Kinoshita, H., Stokking, L.B., and Michael, P.J., eds., Costa Rica Rift, sites 504 and 896: Proceedings of the Ocean Drilling Program, Scientific Results, v. 148, p. 417–434.

Alt, J.C., and Shanks, W.C., III, 2003, Serpentinization of abyssal peridotites from the MARK area, Mid-Atlantic Ridge—Sulfur geochemistry and reaction modeling: Geochimica et Cosmochimica Acta, v. 67, no. 4, p. 641–653.

Alt, J.C., Shanks, W.C., III, Bach, W., Paulick, H., Garrido, C.J., and Beaudoin, G., 2008, Hydrothermal alteration and microbial sulfate reduction in peridotite and gabbro exposed by detachment faulting at the Mid-Atlantic Ridge, 15°20′N (ODP Leg 209)—A sulfur and oxygen isotope study: Geochemistry, Geophysics, Geosystems, v. 8, no. 8, 22 p., doi:10.1029/2007GC001617.

Alt, J.C., and Teagle, D.A.H., 2003, Hydrothermal alteration of upper oceanic crust formed at a fast-spreading ridge—Mineral, chemical, and isotopic evidence from ODP Site 801: Chemical Geology, v. 201, p. 191–211.

Bach, W., and Humphris, S.E., 1999, Relationship between the Sr and O isotope composition of hydrothermal fluids and the spreading and magma-supply rates at oceanic spreading centers: Geology, v. 27, p. 1067–1070.

Baker, P.E., 1982, Evolution and classification of orogenic volcanic rocks, *in* Thorpe, R.S., ed., Andesites—Orogenic andesites and related rocks: New York, John Wiley and Sons, p. 11–23.

Barrie, C.T., and Hannington, M.D., 1999, Classification of volcanic-associated massive sulfide deposits based on host-rock composition, *in* Barrie, C.T., and Hannington, M.D., eds., Volcanic-associated massive sulfide deposits—Processes and examples in modern and ancient settings: Reviews in Economic Geology, v. 8, p. 1–11.

Barriga, F.J.A.S., and Kerrich, R., 1984, Extreme ^{18}O-enriched volcanics and ^{18}O-evolved marine water, Aljustrel, Iberian pyrite belt—Transition from high to low Rayleigh number convective regimes: Geochimica et Cosmochimca Acta, v. 48, p. 1021–1031.

Beaty, D.W., and Taylor, H.P., 1982, Some petrologic and oxygen isotopic relationships in the Amulet Mine, Noranda, Quebec, and their bearing on the origin of Archean massive sulfide deposits: Economic Geology, v. 77, p. 95–108.

Beaty, D.W., Taylor, H.P., Jr., and Coads, P.R., 1988, An oxygen isotope study of the Kidd Creek, Ontario, massive sulfide deposit—Evidence for a ^{18}O ore fluid: Economic Geology, v. 83, p. 1–17.

Boettcher, A.L., and O'Neal, J.R., 1980, Stable isotope, chemical and petrographic studies of high pressure amphiboles and micas—Evidence for metasomatism in the mantle source regions of alkali basalts and kimberslites: American Journal of Science, v. 280-A, p. 594–621.

Cas, R.A.F., 1992, Submarine volcanism—Eruption styles, products, and relevance to understanding the host-rock successions to volcanic-hosted massive sulfide deposits: Economic Geology, v. 87, p. 511–541.

Casey, W.H., and Taylor, B.E., 1982, Oxygen, hydrogen, and sulfur isotope geochemistry of a portion of the West Shasta Cu-Zn District, California: Economic Geology, v. 77, p. 38–49.

Cathles, L.M., 1993, Oxygen alteration in the Noranda Mining District, Abitbi Greenstone Belt, Quebec: Economic Geology, v. 88, p. 1483–1511.

Chester, D.K., Duncan, A.M., Guest, J.E., and Kilburn, C.R.J., 1985, Mount Etna—The anatomy of a volcano: Stanford, Stanford University Press, 404 p.

Costa, U.R., Barnett, R.L., and Kerrich, R., 1983, The Matagami Lake Mine Archean Zn-Cu sulfide deposit, Quebec—Hydrothermal precipitation of talc and sulfides in a sea-floor brine pool—Evidence from geochemistry, $^{18}O/^{16}O$, and sulfide chemistry: Economic Geology, v. 78, p. 1144–1203.

Cotsonika, L.A., Perfit, M.R., Stakes, D., and Ridley, W.I., 2005, The occurrence and origin of andesites and dacites from the southern Juan de Fuca Ridge [abs.]: EOS, Transactions, American Geophysical Union, v. 86, no. 52, Fall meeting supplement, abstract V13B-0551.

Dobson, P.F., Blank, J.G., Maruyama, S., and Liou, J.G., 2006, Petrology and geochemistry of boninite series volcanic rocks, Chichi-jima, Bonin Islands, Japan: International Geology Review, v. 48, p. 669–701.

Duke, N.A., Lindberg, P.A., and West, W.A., in press, Geology of the Greens Creek mining district, *in* Taylor, C.D., and Johnson, C.A., eds., Geology, geochemistry, and genesis of the Greens Creek massive sulfide deposit, Admiralty Island, southeastern Alaska: U.S. Geological Survey Professional Paper 1763.

Dusel-Bacon, C., Wooden, J.L., and Hopkins, M.J., 2004, U-Pb zircon and geochemical evidence for bimodal mid-Paleozoic magmatism and syngenetic base-metal mineralization in the Yukon-Tananaterrane, Alaska: Geological Society of America Bulletin, v. 116, p. 989–1015.

Edmonds, H.N., Michael, P.J., Baker, E.T., Connelly, D.P., Snow, J.E., Langmuir, C.H., Dick, H.J.B., Mühe, R., and German, C.R., 2003, Discovery of abundant hydrothermal venting on the ultraslow-spreading Gakkel ridge in the Arctic Ocean: Nature, v. 421, p. 252–256.

Eiler, J.M, 2001, Oxygen isotope variations of basaltic lavas and upper mantle rocks, *in* Valley, J.W., and Cole, D.R., eds., Stable isotope geochemistry: Reviews in Mineralogy and Geochemistry, v. 43, p. 319–364.

Eiler, J.M., Schiano, P., Kitchen, N., and Stolper, E.M., 2000, Oxygen isotope evidence for recycled crust in the sources of mid-ocean ridge basalts: Nature, v. 403, p. 530–534.

Embley, R.W., Jonasson, I.R., Perfit, M.R., Franklin, J.M., Tivey, M.A., Malahoff, A., Smith, M.F., and Francis, T.J.G, 1988, Submersible investigation of an extinct hydrothermal system on the Galapagos Ridge—Sulfide mounds, stockwork zone, and differentiated lavas: Canadian Mineralogist, v. 26, p. 517–539.

Franklin, J.M., Gibson, H.L., Jonasson, I.R., and Galley, A.G., 2005, Volcanogenic massive sulfide deposits, *in* Hedenquist, J.W., Thompson, J.F.H., Goldfarb, R.J., and Richards, J.P., eds., Economic Geology 100th anniversary volume, 1905–2005: Littleton, Colo., Society of Economic Geologists, p. 523–560.

Galley, A.G., Hannington, M., and Jonasson, I., 2007, Volcanogenic massive sulphide deposits, *in* Goodfellow, W.D., ed., Mineral deposits of Canada—A synthesis of major deposit-types, district metallogeny, the evolution of geological provinces, and exploration methods: Geological Association of Canada, Mineral Deposits Division, Special Publication 5, p. 141–161.

Gamo, T., Ishibashi, J., Tsunogai, U., Okamura, K., and Chiba, H., 2006, Unique geochemistry of submarine hydrothermal fluids from arc-back-arc settings of the western Pacific, *in* Christie, D.M., Fisher, C.R., Lee, S.-M., and Givens, S., eds., Back-arc spreading systems, geological, biological, chemical, and physical interactions: American Geophysical Union, Geophysical Monograph 166, p. 147–161.

Goodfellow, W.D., McCutcheon, S.R., and Peter, J.M., 2003, Introduction and summary of findings, *in* Goodfellow, W.D., McCutcheon, S.R., and Peter, J.M., eds., Massive sulfide deposits of the Bathurst mining camp, New Brunswick, and northern Maine: Economic Geology Monograph 11, p. 1–16.

Green, G.R., Ohmoto, H., Date, J., and Takahashi, T., 1983, Whole-rock oxygen isotope distribution in the Fukazawa-Kosaka area, Hokuroku district, Japan, and its potential application to mineral exploration, *in* Ohmoto, H., and Skinner, B.J., eds., The Kuroko and related volcanogenic massive sulfide deposits: Economic Geology Monograph 5, p. 395–411.

Green, G.R., and Taheri, J., 1992, Stable isotopes and geochemistry as exploration indicators: Geological Survey of Tasmania Bulletin 70, p. 84–91.

Gregory, R.T., and Taylor, H.P., 1981, An oxygen isotope profile in a section of Cretaceous oceanic crust, Samail ophiolite, Oman—Evidence for $\delta^{18}O$ buffering of the oceans by deep (>5 km) seawater-hydrothermal circulation at mid-ocean ridges: Journal of Geophysical Research, v. 86, p. 2737–2755.

Hannington, M.D., Galley, A.G., Herzig, P.M., and Petersen, S., 1998, Comparison of the TAG mound and stockwork complex with Cyprus-type massive sulfide deposits, *in* Herzig, P.M., Humphris, S.E., Miller, D.J., and Zierenberg, R.A., eds., TAG—Drilling an active hydrothermal system on a sediment-free slow-spreading ridge, site 957: Proceedings of the Ocean Drilling Program, Scientific Results, v. 158, p. 389–415.

Harper, G.D., Bowman, J.R., and Kuhns, R., 1988, A field, chemical, and stable isotope study of subseafloor metamorphism of the Josephine ophiolite, California-Oregon: Journal of Geophysical Research, v. 93, p. 4625–4656.

Hattori, K., and Meuhlenbachs, K., 1980, Marine hydrothermal alteration at the Kuroko ore deposit, Kosaka, Japan: Contributions to Mineralogy and Petrology, v. 74, p. 285–292.

Hattori, K., and Sakai, H., 1979, D/H ratios, origins, and evolution of the ore-forming fluids for the Neogene veins and Kuroko deposits of Japan: Economic Geology, v. 74, p. 535–555.

Heaton, T.H.E., and Sheppard, S.M.F., 1977, Hydrogen and oxygen isotope evidence for sea-water-hydrothermal alteration and ore deposition, Troodos comples, Cyprus, *in* Volcanic processes in ore genesis: Institute of Mining and Metallurgy, p. 42–57.

Hoefs, J., 2004, Stable isotope geochemistry: New York, Springer, 244 p.

Holk, G.J., Taylor, B.E., and Galley, A.G., 2008, Oxygen isotope mapping of the Archean Sturgeon Lake caldera complex and VMS-related hydrothermal system, northwestern Ontario, Canada: Mineralium Deposita, v. 43, p. 623–640.

Honma, H., Kusakabe, M., Kagami, H., Iizumi, S., Sakai, H., Kodama, Y., and Kimura, M., 1991, Major and trace element chemistry and D/H, $^{18}O/^{16}O$, $^{87}Sr/^{86}Sr$ and $^{143}Nd/^{144}Nd$ ratios of rocks from the spreading center of the Okinawa Trough, a marginal back-arc basin: Geochemical Journal, v. 25, p. 121–136.

Hoy, L.D., 1993, Regional evolution of hydrothermal fluids in the Noranda District, Quebec—Evidence from $\delta^{18}O$ values from volcanogenic massive sulfide deposits: Economic Geology, v. 88, p. 1526–1541.

Huston, D.L., 1999, Stable isotopes and their significance for understanding the genesis of volcanic-hosted massive sulfide deposits—A review, *in* Barrie, C.T., and Hannington, M.D., eds., Volcanic-associated massive sulfide deposits—Processes and examples in modern and ancient settings: Reviews in Economic Geology, v. 8, p.157–179.

Huston, D.L., and Taylor, B.E., 1999, Genetic significance of oxygen and hydrogen isotope variations at the Kidd Creek volcanic-hosted massive sulfide deposit, Ontario, Canada, *in* Hannington, M.D., and Barrie, C.T., eds., The giant Kidd Creek volcanogenic massive sulfide deposit, western Abitibi subprovince, Canada: Economic Geology Monograph 10, p. 335–350.

Huston, D.L., Taylor, B.E., Bleeker, W., Stewart, B., Cook, R., and Koopman, E.R., 1995, Isotope mapping around the Kidd Creek deposit, Ontario—Application to exploration and comparison with other geochemical indicators: Exploration and Mining Geology, v. 4, p. 175–185.

Ionov, D.A., Hoefs, J., Wedepohl, K.H., and Wiechert, U., 1992, Content and isotopic composition of sulfur in ultramafic xenoliths from central Asia: Earth and Planetary Science Letters, v. 111, p. 269–286.

Ito, E., White, E.M., and Gopel, C., 1987, The O, Sr, Nd and Pb isotope geochemistry of MORB: Chemical Geology, v. 62, p. 157–176.

Jakes, P., and White, A.J.R., 1971, Composition of island arcs and continental growth: Earth and Planetary Science Letters, v. 12, p. 224–230.

Kelley, D.S., Fruh-Green, J.A., Karson, J.A., and Ludwig, K.A., 2007, The Lost City hydrothermal field revisited: Oceanography, v. 20, p. 90–99.

King, E.M., Valley, J.W., and Davis, D.W., 2000, Oxygen isotope evolution of volcanic rocks at the Sturgeon Lake volcanic complex, Ontario: Canadian Journal of Earth Sciences, v. 37, p. 39–50.

Kowalik, J., Rye, R.O., and Sawkins, F.J., 1981, Stable-isotope study of the Buchans, Newfoundland, polymetallic sulfide deposit: Geological Association of Canada Special Paper 22, p. 229–254.

Krasnov, S.G., Cherkashov, G.A., Stepanova, T.V., Batuyev, B.N., Krotov, A.G., Malin, B.V., Maslov, V.F., Poroshina, I.M., Samovarov, M.S., Ashadze, A.M., Lazareva, L.I., and Ermolayev, I.K., 1995a, Detailed geological studies of hydrothermal fields in the North Atlantic, *in* Parsons, L.M., Walker, C.L., and Dixon, D.R., eds., Hydrothermal vents and processes: Geological Society of London Special Publication 87, p. 43–64.

Krasnov, S.G., Proroshina, I.M., and Cherkashev, G.A., 1995b, Geological setting of high-temperature hydrothermal activity and massive sulfide formation on fast and slow-spreading ridges, *in* Parson, L.M., Walker, C.L., and Dixon, D.R., eds., Hydrothermal vents and processes: Geological Society of London Special Publication 87, p. 17–32.

Kyser, T.K., and O'Neal, J.R., 1984, Hydrogen isotope systematics of submarine basalts: Geochimica et Cosmochimica Acta, v. 48, p. 2123–2133.

Langmuir, C.H., Bezos, A., Escrig, S., and Parman, S.W., 2006, Chemical systematics and hydrous melting of the mantle in back-arc basins, *in* Back-arc spreading systems, geological, biological, chemical, and physical interactions: American Geophysical Union, Geophysical Monograph Series 166, p. 87–146.

Large, R.R., 1992, Australian volcanic-hosted massive sulfide deposits—Features, styles, and genetic models: Economic Geology, v. 87, p. 471–510.

Large, R.R., Allen, R.L., Blake, M.D., and Herrmann, W., 2001a, Hydrothermal alteration and volatile element halos for the Rosebery K Lens volcanic-hosted massive sulfide deposit, Western Tasmania: Economic Geology, v. 96, p. 1055–1072.

Large, R.R., Gemmell, J.B., Paulick, H., and Huston, D.L., 2001b, The alteration box plot—A simple approach to understanding the relationship between alteration mineralogy and lithogeochemistry associated with volcanic-hosted massive sulfide deposits: Economic Geology, v. 96, p. 957–971.

Large, R.R., McPhie, J., Gemmell, J.B., Herrmann, W., and Davidson, G.J., 2001c, The spectrum of ore deposit types, volcanic environments, alteration halos, and related exploration vectors in submarine volcanic successions—Some examples from Australia: Economic Geology, v. 96, p. 913–938.

Larson, P.B., 1984, Geochemistry of the alteration pipe at the Bruce Cu-Zn volcanogenic massive sulfide deposit, Arizona: Economic Geology, v. 79, p. 1880–1896.

Le Maitre, R.W., 2002, Igneous rocks—A classification and glossary of terms: Cambridge, Cambridge University Press, 240 p.

Lentz, D.R., 1999, Petrology, geochemistry, and oxygen isotope interpretation of felsic volcanic and related rocks hosting the Brunswick 6 and 12 massive sulfide deposits (Brunswick belt), Bathurst mining camp, New Brunswick, Canada: Economic Geology, v. 84-1A, p. 611–616.

Lowell, R.P., Crowell, B.W., Lewis, K.C., and Liu, L., 2008, Modeling multiphase, multicomponent processes at oceanic spreading centers, *in* Lowell, R.P., Seewald, J.S., Matexas, A., and Perfit, M.R., eds., Magma to microbe—Modeling hydrothermal processes at ocean spreading centers: American Geophysical Union, Geophysical Monograph Series 178, p. 15–44.

Lowell, R.P., Rona, P.A., and Von Herzen, R.P., 1995, Seafloor hydrothermal systems: Journal of Geophysical Research, v. 100, p. 327–352.

Lydon, J.W., 1988, Volcanogenic massive sulfide deposits—Part 2. Genetic models: Geoscience Canada, v. 15, p. 43–65.

MacLean, W.H., and Hoy, L.D., 1991, Geochemistry of hydrothermally altered rocks at the Horne Mine, Noranda, Quebec: Economic Geology, v. 86, p. 506–528.

Maclennan, J., 2008, The supply of heat to mid-ocean ridges by crystallization and cooling of mantle melts, *in* Lowell, R.P., Seewald, J.S., Matexas, A., and Perfit, M.R., eds., Magma to microbe—Modeling hydrothermal processes at ocean spreading centers: American Geophysical Union, Geophysical Monograph Series 178, p. 45–73.

Marumo, K., 1989, Genesis of Kaolin minerals and pyrophyllite in Kuroko deposits of Japan—Implications for the origins of the hydrothermal fluids from mineralogical and stable isotope data: Geochimica et Cosmochimica Acta, v. 53, p. 2915–2924.

Monecke, T., Gemmell, J.B., and Herzig, P.M., 2006, Geology and volcanic facies architecture of the Lower Ordovician Waterloo massive sulfide deposit, Australia: Economic Geology, v. 101, p. 179–197.

Munha, J., Barriga, F.J.A.S., and Kerrich, R., 1986, High ^{18}O ore-forming fluids in volcanic-hosted base metal massive sulfide deposits—Geologic, $^{18}O/^{16}O$, and D/H evidence from the Iberian Pyrite Belt; Crandon, Wisconsin; and Blue Hill, Maine: Economic Geology, v. 81, p. 530–532.

Munha, J., and Kerrich, R., 1980, Sea water basalt interactions in spilites from the Iberian Pyrite Belt: Contributions to Mineralogy and Petrology, v. 73, p. 191–200.

Offler, R., and Whitford, D.J., 1992, Wall-rock alteration and metamorphism of a volcanic-hosted massive sulfide deposit at Que River, Tasmania—Petrology and mineralogy: Economic Geology, v. 87, 686–705.

Ohmoto, H., and Rye, R.O., 1974, Hydrogen and oxygen isotopic composition of fluid inclusions in the Kuroko deposits, Japan: Economic Geology, v. 69, p. 947–953.

Openholzner, J.H., Schroettner, H., Golob, P., and Delgado, H, 2003, Particles from the plume of Popocatepetl volcano, Mexico—The FESEM/EDS approach, *in* Oppenheimer, C., Pyle, D.M., and Barclay, J., eds., Volcanic degassing: Geological Society Special Publication 213, p. 124–148.

Paradis, S., Taylor, B.E., Watkinson, D.H., and Jonasson, I.J., 1993, Oxygen isotope zonation and alteration in the Noranda mining district, Abitibi greenstone belt, Quebec: Economic Geology, v. 88, p. 1512–1525.

Pearce, J.A., 1995, A user's guide to basalt discrimination diagrams, *in* Wyman, D.A., ed., Trace element geochemistry of volcanic rocks—Applications to massive-sulfide exploration: Geological Association of Canada Short Course Notes, v. 12, p. 79–114.

Pearce, J.A., and Cann, J.R., 1973, Tectonic setting of basic volcanic rocks determined using trace element analysis: Earth Planetary Science Letters, v. 19, p. 290–300.

Pearce, J.A., and Peate, D.W., 1995, Tectonic implications of the composition of volcanic arc magmas: Annual Reviews of Earth and Planetary Sciences, v. 23, p. 251–285.

Pearce, J.A., and Stern, R.J., 2006, Origin of back-arc basin magmas—Trace element and isotopic perspectives, *in* Christie, D.M., Fisher, C.R., Lee, S.-M., and Givens, S., eds., Back-arc spreading systems, geological, biological, chemical, and physical interactions: American Geophysical Union, Geophysical Monograph Series 166, p. 63–86.

Perfit, M.R., Ridley, W.I., and Jonasson, I.R., 1999, Geologic, petrologic, and geochemical relationships between magmatism and massive sulfide mineralization at the Eastern Galapagos Spreading Center, *in* Barrie, C.T., and Hannington, M.D., eds., Volcanic-associated massive sulfide deposits—Processes and examples in modern and ancient settings: Reviews in Economic Geology, v. 8, p. 75–100.

Philpotts, A.R., 1990, Principles of igneous and metamorphic petrology: New Jersey, Prentice Hall, 498 p.

Piercey, S.J., 2009, Lithogeochemistry of volcanic rocks associated with volcanogenic massive sulphide deposits and applications to exploration, *in* Cousens, B., and Piercey, S.J., eds., Submarine volcanism and mineralization—Modern through ancient: Geological Association of Canada, Short Course Notes, v. 19, p. 15–40.

Pisutha-Arnond, V., and Ohmoto, H., 1983, Thermal history and chemical and isotopic compositions of the ore-forming fluids responsible for the Kuroko massive sulfide deposits in the Hokuroku District of Japan, *in* Ohmoto, H., and Skinner, B.J., eds., The Kuroko and related volcanogenic massive sulfide deposits: Economic Geology Monograph 5, p. 523–558.

Poorter, R.P.E., Varekamp, J.C., Poreda, R.J., Van Bergen, M.J., and Kreulen, R., 1991, Chemical and isotopic composition of volcanic gases from Sunda and Banda arcs, Indonesia: Geochimica et Cosmochimica Acta, v. 55, p. 3795–3807.

Poreda, R., 1985, Helium-3 and deuterium in back arc basalts—Lau Basin and the Mariana Trough: Earth and Planetary Science Letters, v. 73, p. 244–254.

Poreda, R. J., Schilling, J.-G., and Craig, H., 1986, Helium and hydrogen isotopes in ocean-ridge basalts north and south of Iceland: Earth and Planetary Science Letters, v. 78, p. 1–17.

Ridley, W.I., 1970, The petrology of the Las Canadas volcanoes, Tenerife, Canary Islands: Contributions to Mineralogy and Petrology, v. 26, p. 124–160.

Ridley, W.I., Perfit, M.R., Jonasson, I.R., and Smith, M.F., 1994, Hydrothermal alteration in oceanic ridge volcanic—A detailed study at the Galapagos Fossil Hydrothermal Field: Geochimica et Cosmochimica Acta, v. 58, p. 2477–2494.

Sakai, H., Casadevall, T.J., and Moore, J.G., 1982, Chemistry and isotopic ratios of sulfur in basalts and volcanic gases at Kilauea volcano: Geochimica et Cosmochimica Acta, v. 46, p. 729–738.

Sakai, H., DesMarais, D.J., Ueda, A., and Moore, J.G., 1984, Concentrations and isotope ratios of carbon, nitrogen and sulfur in ocean-floor basalts: Geochimica et Cosmochimica Acta, v. 48, p. 2433–2441.

Schultz, K.J., and Ayuso, R.A., 2003, Lithogeochemistry and paleotectonic setting of the Bald Mountain massive sulfide deposit, northern Maine, *in* Goodfellow, W.D., McCutcheon, S.R., and Peter, J.M., eds., Massive sulfide deposits of the Bathurst mining camp, New Brunswick, and northern Maine: Economic Geology Monograph 11, p. 79–109.

Seyfried, W.E., Jr., Ding, K., Berndt, M.E., and Chen, X., 1999, Experimental and theoretical controls on the compositon of mid-ocean ridge hydrothermal fluids, *in* Barrie, C.T., and Hannington, M.D., eds., Volcanic-associated massive sulfide deposits—Processes and examples in modern and ancient settings: Reviews in Economic Geology, v. 8, p. 181–200.

Shanks, W.C., III, 2001, Stable isotopes in seafloor hydrothermal systems—Vent fluids, hydrothermal deposits, hydrothermal alteration, and microbial processes, *in* Valley, J.W., and Cole, D.R., eds., Stable isotope geochemistry: Reviews in Mineralogy and Geochemistry, v. 43, p. 469–525.

Shanks, W.C., III, Böhlke, J.K., and Seal, R.R., 1995, Stable isotopes in mid-ocean ridge hydrothermal systems—Interactions between fluids, minerals and organisms, *in* Humphris, S.E., Zierenberg, R.A., Mullineaux, L.S., and Thompson, R.E., eds., Seafloor hydrothermal systems—Physical, chemical, biological, and geological interactions: American Geophysical Union, Geophysical Monograph 91, p. 194–221.

Sheppard, S.M.F., 1986, Characterization and isotopic variations in natural waters, *in* Valley, J.W., Taylor, H.P., Jr., and O'Neal, J.R., eds., Stable isotopes: Reviews in Mineralogy, v. 16, p. 165–183.

Singh, S.C., Collier, J.S., Harding, A.J., Kent, G.M., and Orcutt, J.A., 1999, Seismic evidence for a hydrothermal layer above the solid roof of the axial magma chamber at the southern East Pacific Rise: Geology, v. 27, p. 219–222.

Singh, S.C., Crawford, W.C., Carton, H., Seher, T., Combier, V., Cannat, M., Canales, J.P., Düsünür, D., Escartin, J., and Miranda, J.M., 2006, Discovery of a magma chamber and faults beneath a Mid-Atlantic Ridge hydrothermal field: Nature, v. 442, p. 1029–1032.

Sinha, M.C., Contable, S.C., Peirce, C., White, A., Heinson, G., Macgregor, L.M., and Navin, D.A., 1998, Magmatic processes at slow spreading ridges—Implications of the RAMESSES experiment at 57° 45'N on the Mid-Atlantic Ridge: Geophysical Journal International, v. 135, p. 731–745.

Stakes, D.S., and Taylor, H.P., 1992, The northern Samail ophiolite—An oxygen isotope, microprobe, and field study: Journal of Geophysical Research, v. 97, p. 7043–7080.

Stanton, R.L., 1994, Ore elements in arc lavas: Oxford, Oxford Science Publications, 391 p.

Stern, R.J., Fouch, M.J., and Klemperer, S.L., 2003, An overview of the Izu-Bonin-Marianas subduction factory, *in* Eiler, J., ed., Inside the subduction factory: American Geophysical Union, Geophysical Monograph Series 138, p. 175–222.

Stolz, J., and Large, R.R., 1992, Evaluation of the source-rock control on precious metal grades in volcanic-hosted massive sulfide deposits from western Tasmania: Economic Geology, v. 87, p. 720–738.

Taylor, B.E., and Huston, D.L., 1999, Regional ^{18}O zoning and hydrogen isotope studies in the Kidd Creek volcanic complex, Timmins, Ontario, *in* Hannington, M.D., and Barrie, C.T., eds., The giant Kidd Creek volcanogenic massive sulfide deposit, western Abitibi subprovince, Canada: Economic Geology Monograph 10, p. 351–378.

Taylor, B.E., and South, B.C., 1985, Regional stable isotope systematics of hydrothermal alteration and massive sulfide deposition in the West Shasta district, California: Economic Geology, v. 80, p. 2149–2163.

Taylor, H.P., 1974, The application of oxygen and hydrogen isotope studies to problems of hydrothermal alteration and ore deposition: Economic Geology, v. 69, p. 843–883.

Taylor, H.P., 1990, Oxygen and hydrogen isotope constraints on the deep circulation of surface waters into zones of hydrothermal metamorphism and melting, *in* The role of fluids in crustal processes: The National Academies Press; Commission on Geosciences, Environment, and Resources; Geophysics Study Committee, p. 72–95.

Tornos, F., Solomon, M., Conde, C., and Spiro, B.F., 2008, Formation of the Tharsis massive sulfide deposit, Iberian pyrite belt—Geological, lithogeochemical, and stable isotope evidence for deposition in a brine pool: Economic Geology, v. 103, p.185–214.

Urabe, T., and Scott, S.D., 1983, Geology and footwall alteration of the South Bay massive sulfide deposit, northwestern Ontario, Canada: Canadian Journal of Earth Sciences, v. 20, p. 1862–1879.

Urabe, T., Scott, S.D., and Hattori, K., 1983, A comparison of footwall-rock alteration and geothermal systems beneath some Japanese and Canadian volcanogenic massive sulfide deposits, *in* Ohmoto, H., and Skinner, B.J., eds., The Kuroko and related volcanogenic massive sulfide deposits: Economic Geology Monograph 5, p. 345–364.

Veizer, J., Ala, D., Azmy, K., Bruckschen, P., Buhl, D., Bruhn, F., Carden, G.A.F., Dierner, A., Ebneth, S., Godderis, Y., Jasper, T., Korte, C., Pawellek, F., Podlaha, O.G., and Strauss, H., 1999, $^{87}Sr/^{86}Sr$, ^{13}C, ^{18}O evolution of Phanerozoic seawater: Chemical Geology, v. 161, p. 58–88.

Wanless, V.D., Perfit, M.R., Ridley, W.I., and Klein, E., 2010, Dacite petrogenesis on mid-ocean ridges—Evidence for oceanic crustal melting and assimilation: Journal of Petrology, v. 51, p. 2377–2410.

Watanabe, M., and Sakai, H., 1983, Stable isotope geochemistry of sulfates from the Neogene ore deposits of the Green Tuff region, Japan, *in* Ohmoto, H., and Skinner, B.J., eds., The Kuroko and related volcanogenic massive sulfide deposits: Economic Geology Monograph 5, p. 282–291.

Whitford, D.J., Korsch, M.J., and Solomon, M., 1992, Strontium isotope studies of barites—Implications for the origin of base metal mineralization in Tasmania: Economic Geology, v. 87, p. 953–959.

Yang, K., and Scott, S.D., 2006, Magmatic fluids as a source of metals in seafloor hydrothermal systems, *in* Christie, D.M., ed., Back-arc spreading systems—Geological, biological, chemical, and physical interactions: American Geophysical Union, Geophysical Monograph Series 166, p. 163–184.